

Figure 6 Pan-TDP-43 staining of spinal cords of patients with ALS. (A) Autopsied eighth cervical segment of spinal cord immunostained with pan-TDP-43 antibody. Scale bars: 200 μm in A and 50 μm in window insets. (B) Schematic illustration of the distribution of neurons with TDP-43 mislocalization, made by summing data from five sections (at 20- μm intervals). (C) Percentage of neurons with nuclear or cytoplasmic localization of exogenous TDP-43 in the lateral and medial nuclear groups. More frequent TDP-43 mislocalization in the lateral nuclear group in spinal cords of patients with ALS than in the medial nuclear group. Mean \pm SEM, $n = 10$, $P < 0.01$. Scale bars: 50 μm . Lat = lateral nuclear group; Med = ventromedial nuclear group.

transcribed messenger RNA or Flag-TDP protein that is the molecule responsible for this progression, which is a prime objective for our future study.

Bunina bodies are small, cystatin C-positive, eosinophilic cytoplasmic inclusions and are generally considered a specific hallmark of sporadic ALS (Okamoto *et al.*, 1993; Mitsumoto *et al.*, 1998). Importantly, Bunina bodies are absent in familial ALS that is due to the SOD1 mutation (Tan *et al.*, 2007) or FUS/TLS mutation (Tateishi *et al.*, 2010), but they have been detected in familial ALS with the TDP-43 mutation (Yokoseki *et al.*, 2008) as well as in sporadic ALS. These imply an association between Bunina bodies and TDP-43 pathology in sporadic ALS. From this point of view, the generation of cystatin C-positive cytoplasmic aggregates in our monkeys might strengthen their pathological value as a model of sporadic ALS.

Biochemically, TDP-43 proteinopathy is characterized by decreased solubility, phosphorylation and the generation of 25-kDa C-terminal fragment (Arai *et al.*, 2006; Neumann *et al.*,

2006; Hasegawa *et al.*, 2008). In TDP-43-overexpressing monkeys, the exogenous TDP-43 became much more insoluble than endogenous TDP-43 of control monkeys, indicating that expression of large amounts of exogenous wild-type TDP-43 can render it insoluble. Unexpectedly, the solubility of endogenous monkey TDP-43 did not become insoluble in TDP-43-overexpressing monkeys. The expectation would be that exogenous insoluble TDP-43 would recruit endogenous monkey TDP-43 and alter its solubility. In this biochemical aspect of TDP-43 solubility, our monkey model differs from patients with ALS.

The pathological role of phosphorylated TDP-43 is still unclear; TDP-43 phosphorylation in culture cells enhances its oligomerization (Hasegawa *et al.*, 2008), but experiments with a phosphorylation-resistant mutant TDP-43 indicated that phosphorylation is not required for inclusion formation or cellular toxicity (Zhang *et al.*, 2009). In our monkeys, phosphorylation of TDP-43 was a late event but not observed at 4 days after symptom onset. This finding suggests that TDP-43 phosphorylation is not

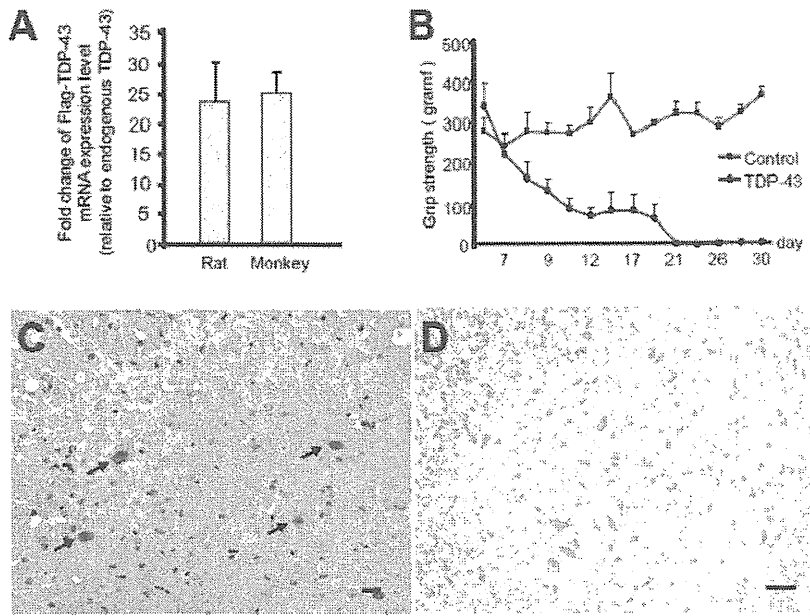


Figure 7 Effect of TDP-43-expressing AAV in rat spinal cords. (A) Ratio of exogenously expressed Flag-TDP-43 messenger RNA level to endogenous rat or cynomolgus TDP-43 messenger RNA level evaluated by quantitative real-time polymerase chain reaction. Mean \pm SEM, rat, $n = 4$; cynomolgus, $n = 3$, $P = 0.74$. (B) Time course of grip strength. Mean \pm SEM. (C) Nuclear staining of exogenous TDP-43 in cervical cord sections of AAV-injected rats by immunostaining with an anti-Flag antibody (arrows). (D) Immunostaining of cervical cord sections of TDP-43-expressing rat, 4 weeks after injection, with SM131 did not show aberrant phosphorylated neurofilament in the neuronal cytoplasm. Scale bars: 20 μ m.

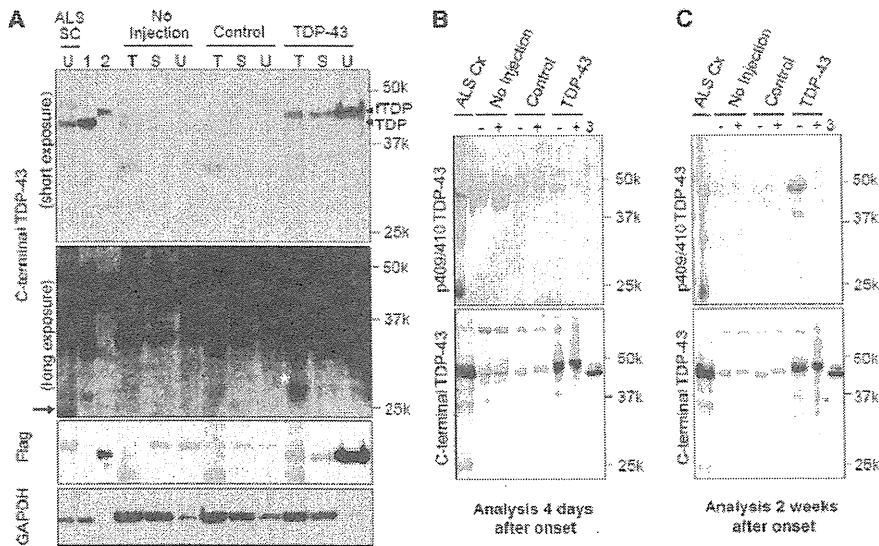


Figure 8 Biochemical analysis of monkey spinal cords. (A) Immunoblot of cervical spinal cord lysates from TDP-43-expressing monkeys (4 weeks after injection) and patients with ALS using antibodies recognizing the C-terminus of TDP-43 and Flag. SC = spinal cord of patient with ALS; 1 = TDP-43-expressing HEK 293 T cell lysate; 2 = Flag-TDP-43-expressing HEK 293T cell lysate; T = 1% Triton X-100-soluble; S = 1% sarkosyl-soluble; U = 8 mol/l urea-soluble fraction; fTDP = Flag-TDP-43. A longer exposure (second panel from top) revealed the 25-kDa C-terminal fragment in the spinal cord of a patient with ALS (arrow). The \sim 30-kDa band noted in the Triton-soluble fraction from the spinal cord of a TDP-43-expressing monkey (asterisk) was different from the 25-kDa C-terminal fragment (arrow). (B and C) Immunoblot of 8 mol/l urea-soluble fraction from the monkey spinal cord harvested 4 days (B) and 2 weeks (C) after onset of symptoms, using antibodies to pS409/410 TDP-43 (top) and C-TDP-43 (bottom) before (–) and after (+) treatment with lambda protein phosphatase (λ PPase). 3 = Mixture of Flag-TDP-43- and TDP-43-expressing HEK 293T cell lysates. The phosphorylated TDP-43 was detected only in the late stage (asterisk).

necessary to initiate motor symptoms and is a late event in motoneuron degeneration.

In the spinal cords of our monkeys, neither a C-terminal nor a phosphospecific TDP-43 antibody detected the 25-kDa C-terminal fragment that is found in patients with ALS. Overexpressed 25-kDa C-terminal fragment in cultured cells is reported to be toxic (Igaz *et al.*, 2009; Zhang *et al.*, 2009), and the accumulation of 25-kDa C-terminal fragment in transgenic mouse brain correlates with disease progression (Xu *et al.*, 2010). Interestingly, unlike the FTL/ALS brain, the 25-kDa C-terminal fragment is often absent in the ALS spinal cord (Neumann *et al.*, 2009). The absence of 25-kDa C-terminal fragment in ALS spinal cord does not necessarily preclude a primary role for this form; rather it can be pathologically crucial if its absence is due to the accelerated degeneration of motoneurons with 25-kDa C-terminal fragment. It is difficult to deny that small amounts of C-terminal truncated species are actually present, because mislocalization of TDP-43 was focal in the spinal cord of our monkeys. However, the failure to detect 25-kDa C-terminal fragment in our monkey spinal cord at the early stage may have an implication that full-length TDP-43 is sufficient to be toxic, because α -motor axonal excitability was impaired but their cell bodies were preserved at autopsy.

The results of studies on the relationship between TDP-43 mislocalization and neuron loss remain controversial. The overexpression of wild-type TDP-43 in the nuclei in a transgenic rodent model was sufficient to be toxic to spinal motoneurons (Li *et al.*, 2010; Shan *et al.*, 2010; Wils *et al.*, 2010; Xu *et al.*, 2010), which is consistent with our observations in the rat model. In this context, it can be interpreted that the cytoplasmic mislocalization of wild-type TDP-43 is an epiphenomenon and not a necessary condition for the disease. However, in our monkey model, TDP-43 mislocalization was detected in almost all of the large motoneurons of the lateral nuclear group at the early or even the presymptomatic stage, and these motoneurons later showed neuron loss. In contrast, overexpressed exogenous TDP-43 in the large motoneurons of the ventromedial nuclear group was restricted to the nucleus, but did not produce neuron loss. Mice with over-expression of human TDP-43 engineered to localize in the cytoplasm showed progressive neuronal loss and downregulation of endogenous nuclear mouse TDP-43 expression (Igaz *et al.*, 2011). These suggest that TDP-43 mislocalization is an upstream event in the cascade of motoneuronal degeneration. This finding is consistent with the observation that the highest percentage of neurons with TDP-43 mislocalization was found in the early stage of ALS in patients (Giordana *et al.*, 2010).

In conclusion, our monkey model is superior to rodent models in recapitulating the TDP-43 pathology and in the presence of Bunina body-like inclusion and is expected to be a powerful tool for investigating developing effective therapies as well as the disease pathogenesis of sporadic ALS.

Acknowledgements

The authors are grateful to Drs Masato Hasegawa, Makoto Urushitani and Hiroshi Tsukagoshi for discussion and technical advices on Western blotting and pathological analysis; Dr

Takashi Shimada, and Ms Fumiko Sunaga for AAV preparation; Dr Satoshi Ikeda, Dr Masumi Ichikawa, Dr Kinya Ishikawa, Miss Tomoko Ueno, Miss Minako Suzuki, Ms Michiko Imanishi, and Ms Hiromi Kondo for technical support on pathological analysis; Dr Kazuo Kusano for surgical support; Ms Yuki Yamamoto, Dr Miho Akaza for their help.

Funding

Comprehensive Research on Disability Health and Welfare (Grant Nos 20301501 and 23161501 to T.Y. and H.M.); Research on Neurodegenerative Diseases/ALS from Ministry of Health, Labor and Welfare, Japan; Grant-in-Aid for Scientific Research (A) (Grant No. 22240039 to T.Y.) and Grant-in-Aid for Research Activity Start-up (Grant No. 22890051 to T.T.) and Strategic Research Program for Brain Science, Field E from Ministry of Education, Culture, Sports and Technology, Japan.

Supplementary material

Supplementary material is available at *Brain* online.

References

- Anderson KD, Gunawan A, Steward O. Spinal pathways involved in the control of forelimb motor function in rats. *Exp Neurol* 2005; 194: 161–74.
- Arai T, Hasegawa M, Akiyama H, Ikeda K, Nonaka T, Mori H, et al. TDP-43 is a component of ubiquitin-positive tau-negative inclusions in frontotemporal lobar degeneration and amyotrophic lateral sclerosis. *Biochem Biophys Res Commun* 2006; 351: 602–11.
- Ash PE, Zhang YJ, Roberts CM, Saldi T, Hutter H, Buratti E, et al. Neurotoxic effects of TDP-43 overexpression in *C. elegans*. *Hum Mol Genet* 2010; 19: 3206–18.
- Ayala YM, De Conti L, Avendaño-Vázquez SE, Dhir A, Romano M, D'Ambrogio A, et al. TDP-43 regulates its mRNA levels through a negative feedback loop. *EMBO J* 2011; 30: 277–88.
- Bisland LG, Sahai E, Kelly G, Golding M, Greensmith L, Schiavo G. Deficits in axonal transport precede ALS symptoms in vivo. *Proc Natl Acad Sci USA* 2010; 107: 20523–8.
- Brooks BR, Miller RG, Swash M, Munsat TL. El Escorial revisited: revised criteria for the diagnosis of amyotrophic lateral sclerosis. *Amyotroph Lateral Scler Other Motor Neuron Disord* 2000; 1: 293–9.
- Buratti E, Baralle FE. Characterization and functional implications of the RNA binding properties of nuclear factor TDP-43, a novel splicing regulator of CFTR exon 9. *J Biol Chem* 2001; 276: 36337–43.
- Buratti E, Baralle FE. Multiple roles of TDP-43 in gene expression, splicing regulation, and human disease. *Front Biosci* 2008; 13: 867–8.
- Buratti E, De Conti L, Stuani C, Romano M, Baralle M, Baralle F. Nuclear factor TDP-43 can affect selected microRNA levels. *FEBS J* 2010; 277: 2268–81.
- Cairns NJ, Neumann M, Bigio EH, Holm IE, Troost D, Hatanpaa KJ, et al. TDP-43 in familial and sporadic frontotemporal lobar degeneration with ubiquitin inclusions. *Am J Pathol* 2007; 171: 227–40.
- Carpenter MB, Sutin J. *Human neuroanatomy*. 8th edn. Baltimore: Williams & Wilkins; 1983.
- Corbo M, Hays AP. Peripherin and neurofilament protein coexist in spinal spheroids of motor neuron disease. *J Neuropathol Exp Neurol* 1992; 51: 531–7.

- De Carvalho M, Dengler R, Eisen A, England JD, Kaji R, Kimura J, et al. Electrodiagnostic criteria for diagnosis of ALS. *Clin Neurophysiol* 2008; 119: 497–503.
- Dengler R, Konstanzer A, Küther G, Hesse S. Amyotrophic lateral sclerosis: Macro-EMG and twitch forces of single motor units. *Muscle Nerve* 1990; 13: 545–50.
- Geser F, Lee VM, Trojanowski JQ. Amyotrophic lateral sclerosis and frontotemporal lobar degeneration: A spectrum of TDP-43 proteinopathies. *Neuropathology* 2010; 30: 103–12.
- Giordana MT, Piccinini M, Grifoni S, De Marco G, Vercellino M, Magistrello M, et al. TDP-43 redistribution is an early event in sporadic amyotrophic lateral sclerosis. *Brain Pathol* 2010; 20: 351–60.
- Gitcho MA, Bigio EH, Mishra M, Johnson N, Weintraub S, Mesulam M, et al. TARDBP 3'-UTR variant in autopsy-confirmed frontotemporal lobar degeneration with TDP-43 proteinopathy. *Acta Neuropathol* 2009; 11: 633–45.
- Hanson KA, Kim SH, Wassarman DA, Tibbetts RS. Ubiquitin modifies TDP-43 toxicity in a *Drosophila* model of amyotrophic lateral sclerosis (ALS). *J Biol Chem* 2010; 285: 11068–72.
- Harverkamp LJ, Appel V, Appel SH. Natural history of amyotrophic lateral sclerosis in a data base population. Validation of a scoring system and a model for survival prediction. *Brain* 1995; 118: 707–19.
- Hasegawa M, Arai T, Nonaka T, Kametani F, Yoshida M, Hashizume Y, et al. Phosphorylated TDP-43 in frontotemporal lobar degeneration and amyotrophic lateral sclerosis. *Ann Neurol* 2008; 64: 60–70.
- Igaz LM, Kwong LK, Chen-Plotkin A, Winton MJ, Unger TL, Xu Y, et al. Expression of TDP-43 C-terminal fragments in vitro recapitulates pathological features of TDP-43 proteinopathies. *J Biol Chem* 2009; 284: 8516–24.
- Igaz LM, Kwong LK, Lee EB, Chen-Plotkin A, Swanson E, Unger T, et al. Dysregulation of the ALS-associated gene TDP-43 leads to neuronal death and degeneration in mice. *J Clin Invest* 2011; 121: 726–38.
- Kabashi E, Lin L, Tradewell ML, Dion PA, Bercier V, Bourgouin P, et al. Gain and loss of function of ALS-related mutations of TARDBP (TDP-43) cause motor deficits in vivo. *Hum Mol Genet* 2010; 19: 671–83.
- Kabashi E, Valdmanis PN, Dion P, Spiegelman D, McConkey BJ, Vande Velde C, et al. TARDBP mutations in individuals with sporadic and familial amyotrophic lateral sclerosis. *Nat Genet* 2008; 40: 572–4.
- Körner S, Kollwe K, Fahlbusch M, Zapf A, Dengler R, Krampfl K, et al. Onset and spreading patterns of upper and lower motor neuron symptoms in amyotrophic lateral sclerosis. *Muscle Nerve* 2011; 43: 636–42.
- Li Y, Ray P, Rao EJ, Shi C, Guo W, Chen X, et al. A *Drosophila* model for TDP-43 proteinopathy. *Proc Natl Acad Sci USA* 2010; 107: 3169–74.
- Mackenzie IRA, Neumann M, Baborie A, Sampathu DM, Plessis DD, Jaros E, et al. A harmonized classification system for FTLD-TDP pathology. *Acta Neuropathol* 2011; 122: 111–3.
- Mishra M, Paunesku T, Woloschak GE, Siddique T, Zhu LJ, Lin S, et al. Gene expression analysis of frontotemporal lobar degeneration of the motor neuron disease type with ubiquitinated inclusions. *Acta Neuropathol* 2007; 114: 81–94.
- Mitsumoto H, Chad DA, Piro EP. Amyotrophic lateral sclerosis. Philadelphia: F.A. Davis; 1998.
- Munoz DG, Greene C, Perl DP, Selkoe DJ. Accumulation of phosphorylated neurofilaments in anterior horn motoneurons of amyotrophic lateral sclerosis patients. *J Neuropathol Exp Neurol* 1988; 47: 9–18.
- Neumann M, Kwong LK, Lee EB, Kremmer E, Flatley A, Xu Y, et al. Phosphorylation of S409/410 of TDP-43 is a consistent feature in all sporadic and familial forms of TDP-43 proteinopathies. *Acta Neuropathol* 2009; 117: 137–49.
- Neumann M, Sampathu DM, Kwong LK, Truax AC, Micsenyi MC, Chou TT, et al. Ubiquitinated TDP-43 in frontotemporal lobar degeneration and amyotrophic lateral sclerosis. *Science* 2006; 314: 130–3.
- Okamoto K, Hirai S, Amari M, Watanabe M, Sakurai A. Bunina bodies in amyotrophic lateral sclerosis immunostained with rabbit anti-cystatin C serum. *Neurosci Lett* 1993; 162: 125–8.
- Ou SH, Wu F, Harrich D, Garcia-Martinez LF, Gaynor RB. Cloning and characterization of a novel cellular protein, TDP-43, that binds to human immunodeficiency virus type 1 TAR DNA sequence motifs. *J Virol* 1995; 69: 3584–96.
- Piao YS, Wakabayashi K, Kakita A, Yamada M, Hayashi S, Morita T, et al. Neuropathology with clinical correlations of sporadic amyotrophic lateral sclerosis: 102 autopsy cases examined between 1962 and 2000. *Brain Pathol* 2003; 13: 10–22.
- Polymenidou M, Lagier-Tourenne C, Hutt KR, Huelga SC, Moran J, Liang TY, et al. Long pre-mRNA deletion and RNA missplicing contribute to neuronal vulnerability from loss of TDP-43. *Nat Neurosci* 2011; 14: 459–68.
- Pun S, Santos AF, Saxena S, Xu L, Caroni P. Selective vulnerability and pruning of phasic motoneuron axons in motoneuron disease alleviated by CNTF. *Nat Neurosci* 2006; 9: 408–19.
- Shan X, Chiang PM, Price DL, Wong PC. Altered distributions of gemini of coiled bodies and mitochondria in motor neurons of TDP-43 transgenic mice. *Proc Natl Acad Sci USA* 2010; 107: 16325–30.
- Swarup V, Phaneuf D, Bareil C, Robertson J, Rouleau GA, Kriz J, et al. Pathological hallmarks of amyotrophic lateral sclerosis/frontotemporal lobar degeneration in transgenic mice produced with TDP-43 genomic fragments. *Brain* 2011; 134: 2610–26.
- Tan CF, Eguchi H, Tagawa A, Onodera O, Iwasaki T, Tsujino A, et al. TDP-43 immunoreactivity in neuronal inclusions in familial amyotrophic lateral sclerosis with or without SOD1 gene mutation. *Acta Neuropathol* 2007; 113: 535–42.
- Tateishi T, Hokenohara T, Yamasaki R, Miura S, Kikuchi H, Iwaki A, et al. Multiple system degeneration with basophilic inclusions in Japanese ALS patients with FUS mutation. *Acta Neuropathol* 2010; 119: 355–64.
- Voigt A, Herholz D, Fiesel FC, Kaur K, Müller D, Karsten P, et al. TDP-43-mediated neuron loss in vivo requires RNA-binding activity. *PLoS ONE* 2010; 5: e12247.
- Wils H, Kleinberger G, Janssens J, Pereson S, Joris G, Cuijt I, et al. TDP-43 transgenic mice develop spastic paralysis and neuronal inclusions characteristic of ALS and frontotemporal lobar degeneration. *Proc Natl Acad Sci USA* 2010; 107: 3858–63.
- Xu YF, Gendron TF, Zhang YJ, Lin WL, D'Alton S, Sheng H, et al. Wild-type human TDP-43 expression causes TDP-43 phosphorylation, mitochondrial aggregation, motor deficits, and early mortality in transgenic mice. *J Neurosci* 2010; 30: 10851–9.
- Yokoseki A, Shiga A, Tan CF, Tagawa A, Kaneko H, Koyama A, et al. TDP-43 mutation in familial amyotrophic lateral sclerosis. *Ann Neurol* 2008; 63: 538–42.
- Zhang YJ, Xu YF, Cook C, Gendron TF, Roettges P, Link CD, et al. Aberrant cleavage of TDP-43 enhances aggregation and cellular toxicity. *Proc Natl Acad Sci USA* 2009; 106: 7607–12.

Geographical, genetic and functional diversity of antiretroviral host factor TRIMCyp in cynomolgus macaque (*Macaca fascicularis*)

Akatsuki Saito,^{1†} Ken Kono,^{2†} Masako Nomaguchi,³ Yasuhiro Yasutomi,⁴ Akio Adachi,³ Tatsuo Shioda,² Hirofumi Akari^{1,4} and Emi E. Nakayama²

Correspondence

Hirofumi Akari
akari@pri.kyoto-u.ac.jp
Emi E. Nakayama
emien@biken.osaka-u.ac.jp

¹Primate Research Institute, Kyoto University, Inuyama 484-8506, Japan

²Department of Viral Infections, Research Institute for Microbial Diseases, Osaka University, Suita 565-0871, Japan

³Department of Microbiology, Institute of Health Biosciences, The University of Tokushima Graduate School, Tokushima 770-8503, Japan

⁴Tsukuba Primate Research Center, National Institute of Biomedical Innovation, Tsukuba 305-0843, Japan

The antiretroviral factor tripartite motif protein 5 (*TRIM5*) gene-derived isoform (TRIMCyp) has been found in at least three species of Old World monkey: rhesus (*Macaca mulatta*), pig-tailed (*Macaca nemestrina*) and cynomolgus (*Macaca fascicularis*) macaques. Although the frequency of TRIMCyp has been well studied in rhesus and pig-tailed macaques, the frequency and prevalence of TRIMCyp in cynomolgus macaques remain to be definitively elucidated. Here, the geographical and genetic diversity of TRIM5 α /TRIMCyp in cynomolgus macaques was studied in comparison with their anti-lentiviral activity. It was found that the frequency of TRIMCyp in a population in the Philippines was significantly higher than those in Indonesian and Malaysian populations. Major and minor haplotypes of cynomolgus macaque TRIMCyp with single nucleotide polymorphisms in the cyclophilin A domain were also found. The functional significance of the polymorphism in TRIMCyp was examined, and it was demonstrated that the major haplotype of TRIMCyp suppressed human immunodeficiency virus type 1 (HIV-1) but not HIV-2, whilst the minor haplotype of TRIMCyp suppressed HIV-2 but not HIV-1. The major haplotype of TRIMCyp did not restrict a monkey-tropic HIV-1 clone, NL-DT5R, which contains a capsid with the simian immunodeficiency virus-derived loop between α -helices 4 and 5 and the entire *vif* gene. These results indicate that polymorphisms of TRIMCyp affect its anti-lentiviral activity. Overall, the results of this study will help our understanding of the genetic background of cynomolgus macaque TRIMCyp, as well as the host factors composing species barriers of primate lentiviruses.

Received 2 October 2011

Accepted 22 November 2011

INTRODUCTION

Human immunodeficiency virus type 1 (HIV-1) barely replicates in Old World monkeys such as cynomolgus macaques (CMs; *Macaca fascicularis*) and rhesus macaques (RMs; *Macaca mulatta*). This species barrier has long hampered the use of Old World monkeys for human immunodeficiency virus type 1 (HIV-1) research. Recently, a number of intrinsic anti-HIV-1 cellular factors, including

tripartite motif protein 5 α (TRIM5 α), cyclophilin A (CypA), the apolipoprotein B mRNA-editing enzyme catalytic polypeptide-like 3 (APOBEC3) family and tetherin were identified in Old World monkey cells (Nomaguchi *et al.*, 2008; Sauter *et al.*, 2010). Of these factors, TRIM5 α was found to strongly suppress HIV-1 replication, mainly by affecting the virus disassembly step, resulting in a decrease in reverse-transcription products (Nakayama & Shioda, 2010; Stremlau *et al.*, 2004). TRIM5 α contains a RING domain, a B-box domain, a coiled-coil domain and a PRYSPRY (B30.2) domain. Importantly, the PRYSPRY domain recognizes the capsid of incoming retroviruses, leading to post-entry restriction of infection. RM and CM TRIM5 α restrict HIV-1 but not simian immunodeficiency virus isolated from an infected rhesus macaque (SIVmac) (Nakayama *et al.*, 2005; Stremlau *et al.*, 2004; Yap *et al.*, 2004). In the case of HIV-2

†These authors contributed equally to this work.

The GenBank/EMBL/DDBJ accession numbers for the sequences of CM TRIMCyp-major (DK) and RM TRIMCyp are AB671588 and AB671589, respectively.

Two supplementary tables are available with the online version of this paper.

infection, viruses carrying proline (P) at aa 120 of the capsid protein are sensitive to CM TRIM5 α , whereas those with either alanine or glutamine (Q) are resistant (Song *et al.*, 2007). Both CM TRIM5 α -sensitive and -resistant HIV-2 strains are restricted by RM TRIM5 α , and three amino acid residues – threonine (T), phenylalanine (F) and P at aa 339, 340 and 341, respectively – of RM TRIM5 α are important for restricting particular HIV-2 strains, which are still resistant to CM TRIM5 α (Kono *et al.*, 2008). It is also known that TRIM5 α exhibits a high degree of sequence variation, even within macaque species. In some individual RMs, the TFP residues at aa 339–341 of TRIM5 α are replaced with a single Q (Newman *et al.*, 2006) and this TFP→Q polymorphism affects the anti-lentiviral activity of RM TRIM5 α (Kirmaier *et al.*, 2010).

Although pig-tailed macaques (PMs; *Macaca nemestrina*) have long been thought to exhibit a higher susceptibility to HIV-1 infection than RMs and CMs (Agy *et al.*, 1992), the underlying mechanism determining this difference remained unclear. Recently, a TRIM5–CypA chimeric protein, referred to as TRIMCyp, was discovered in PMs, and the monkeys exclusively expressed TRIMCyp but not TRIM5 α (Brennan *et al.*, 2008; Liao *et al.*, 2007). TRIMCyp is an alternatively spliced isoform of the *TRIM5* gene in which the PRYSPRY domain of TRIM5 α is replaced with a retrotransposed *CypA* gene. The retrotransposition of the *CypA* sequence in the 3' UTR of the *TRIM5* gene correlates with a single nucleotide polymorphism (SNP) at the exon 7 splice-acceptor site, leading to skipping of exons 7 and 8 encoding the PRYSPRY domain and splicing to the *CypA* insertion. Thus, the presence or absence of the *CypA* sequence in the 3' UTR results in expression of TRIMCyp or TRIM5 α , respectively.

In vitro analyses demonstrated that cells expressing PM TRIMCyp restricted HIV-2 but not HIV-1 infection (Brennan *et al.*, 2008; Liao *et al.*, 2007), suggesting that the characteristic isoform of the *TRIM5* gene in PMs may be one of the reasons for their greater susceptibility to HIV-1 infection. Furthermore, TRIMCyp was also identified in some individual RMs and CMs (Brennan *et al.*, 2008; Newman *et al.*, 2008; Wilson *et al.*, 2008a). RM TRIMCyp, as well as that of PMs, is unable to restrict HIV-1 infection (Wilson *et al.*, 2008a). This report also showed that the frequency of TRIMCyp in Indian RMs was approximately 25%, whilst it was not found in the Chinese RM population, suggesting a geographical deviation in the frequency of TRIMCyp (Wilson *et al.*, 2008a). In the case of CMs, although the existence of TRIMCyp has been reported (Brennan *et al.*, 2008), the allele frequency, geographical distribution and relevance in antiviral activity of TRIMCyp remain to be elucidated. As the *TRIM5* gene-related factors are expected to have an impact on the replication of retroviruses, information about the genetic background of CM TRIMCyp will contribute to our understanding of host factors composing the species barrier. In the present study, we studied the geographical, genetic and functional diversity of CM TRIMCyp originating from South-West Asia (Indonesia, Malaysia and the Philippines). We showed a geographical deviation in the frequency of

TRIMCyp. Moreover, we found SNPs in CM TRIMCyp and analysed their impact on the anti-lentiviral functions, including their effect against HIV-1, HIV-2, SIVmac and monkey-tropic HIV-1 (HIV-1mt).

RESULTS

Geographical deviation in the frequency of CM TRIMCyp

Initially, we analysed the frequencies of TRIM5 α and TRIMCyp genotypes in 126 CMs originating from three different regions – Indonesia, Malaysia and the Philippines – using a PCR-based assay designed to differentiate between the presence and absence of the *CypA* insertion (Fig. 1a) (Wilson *et al.*, 2008a). Insertion of the *CypA* gene in TRIMCyp resulted in a PCR product larger than the expected size for TRIM5 α (Fig. 1b).

As shown in Table 1, 35 of the 46 Philippine individuals were homozygous for TRIMCyp, ten were heterozygous and only one was homozygous for TRIM5 α . In contrast, only three of the 33 Indonesian individuals were homozygous for TRIMCyp, 17 were heterozygous and 13 were homozygous for TRIM5 α . Interestingly, the Malaysian population was of intermediate proportions: ten TRIMCyp homozygotes, 26 heterozygotes and 11 TRIM5 α homozygotes. As shown in Fig. 2, the percentages of individuals having each *TRIM5* genotype indicated that the frequency of TRIMCyp homozygotes in Malaysian CMs was twice that in Indonesian CMs. In contrast, the frequency of TRIM5 α homozygotes in Indonesian CMs was twice that in Malaysian CMs. Taken together, the calculated allele frequencies of TRIMCyp in the Philippine, Indonesian and Malaysian CM populations were 87.0, 34.8 and 48.9%, respectively (Table 1). Statistical analyses using a χ^2 test followed by Bonferroni correction demonstrated that the frequency of TRIMCyp in the Philippine population was significantly higher than that in the Indonesian ($P < 0.0001$) and Malaysian ($P < 0.0001$) populations. In contrast, there was no significant difference between the Indonesian and Malaysian populations ($P = 0.2295$).

It should be noted that our method failed to distinguish homozygotes from hemizygotes, especially when the subjects exhibited no polymorphisms in the *TRIM5* gene. However, hemizygosity for the *TRIM5* gene is highly unlikely for the following reasons: (i) the *TRIM5* gene is on an autosomal chromosome, (ii) there is no precedent of deletion of the *TRIM5* gene in humans or primates, and (iii) all of the three CM populations in Table 1 are in Hardy–Weinberg equilibrium for *TRIM5* genotypes.

Polymorphisms in the *CypA* domain of CM TRIMCyp

Previously, it was reported that aa 357 of CM TRIMCyp, corresponding to aa 54 counting from the methionine of

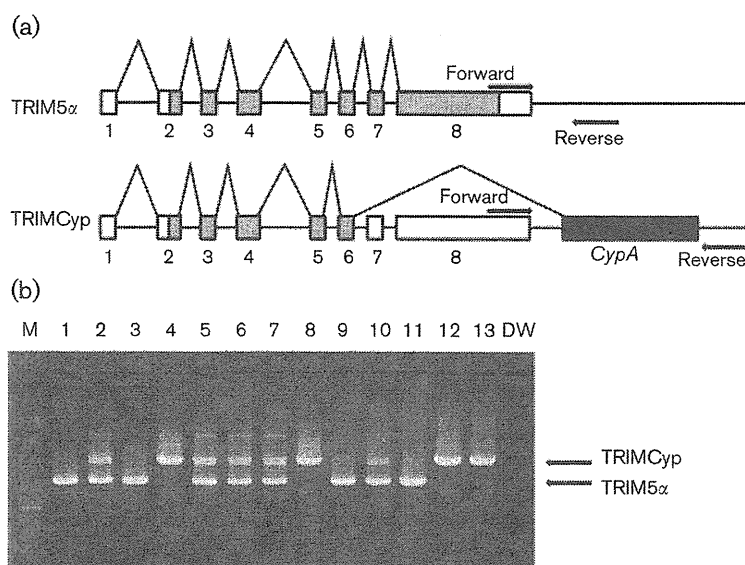


Fig. 1. Determination of *CypA* insertion. (a) Diagram indicating the splicing of *TRIM5 α* or *TRIMCyp*. Non-coding and coding exons (numbered) and *CypA* sequences are indicated as open, shaded and filled boxes, respectively. The primers used in this study are indicated by arrows. (b) Genomic DNA was extracted from PBMCs. To test for *CypA* insertion, the 3' region of the *TRIM5* gene was amplified by PCR with primers spanning the 3' UTR and the putative *CypA* insertion. DW, Distilled water control.

CypA, was arginine (R) (Brennan *et al.*, 2008). Subsequently, Ylinen *et al.* (2010) reported another allele of CM *TRIMCyp* encoding histidine (H) at this position. To determine the frequency of this R→H polymorphism, we examined 34 *TRIM5 α /TRIMCyp* heterozygotes and 30 *TRIMCyp* homozygotes for sequence variations in the *CypA* domain. The results showed that there was no *TRIMCyp* allele encoding R at position 357 (*Cyp* 54R). All 94 CM chromosomes carrying the *TRIMCyp* gene encoded *TRIMCyp* with H at this position. This result was consistent with the results reported recently by Dietrich *et al.* (2011).

Dietrich *et al.* (2011) also reported CM *TRIMCyp* polymorphisms at aa 369 and 446, corresponding to aa 66 and 143 in the *CypA* domain, respectively. Both Brennan *et al.* (2008) and Ylinen *et al.* (2010) reported that aa 369 (*Cyp*66) and 446 (*Cyp*143) are aspartic acid (D) and lysine (K), respectively (denoted as the DK haplotype), whilst Dietrich *et al.* (2011) showed the presence of another haplotype encoding asparagine (N) and glutamic acid (E) at positions 369 (*Cyp*66) and 446 (*Cyp*143), respectively (denoted as the NE haplotype). Our results showed that 12 CM chromosomes carried *TRIMCyp* with the NE haplotype, whilst the remaining 82 *TRIMCyp* were all the DK haplotype (Table 2). Residues 369N (*Cyp* 66N) and 446E (*Cyp* 143E) were also

found in PM and RM *TRIMCyps*, and the *CypA* portion of the NE haplotype of CM *TRIMCyp* has the same amino acid sequence as RM *TRIMCyp* (GenBank accession no. EU157763). These results indicate that the previously recognized interspecies variations of the *CypA* sequence of *TRIMCyp* were in fact intraspecies variation within CMs. With respect to the geographical distribution of these haplotypes, we found no significant deviation in the frequencies of the haplotypes among the three origins (Table 2).

Polymorphisms in the RING, B-box, coiled-coil, linker and PRYSPRY domains of CM *TRIM5 α* and *TRIMCyp*

To identify polymorphisms that are in possible linkage disequilibrium with either the DK or NE haplotype in regions other than the *CypA* domain, we determined nucleotide sequences of *TRIM5 α* and *TRIMCyp* cDNAs encoding the RING, B-box, coiled-coil and linker domains of six *TRIMCyp* homozygotes (three homozygotes of the DK haplotype and three heterozygotes for the DK and NE haplotypes) and three *TRIM5 α* homozygotes (see Supplementary Table S1, available in JGV Online). We found polymorphisms at positions 4 [E→glycine (G)] in

Table 1. Frequencies of *TRIMCyp* alleles in CM populations

Origin	No. of animals	Genotype (no. of animals)			Allele frequency (%)	
		<i>TRIM5α</i> homozygote	<i>TRIM5α/TRIMCyp</i> heterozygote	<i>TRIMCyp</i> homozygote	<i>TRIM5α</i>	<i>TRIMCyp</i>
Philippines	46	1	10	35	13.0	87.0
Malaysia	47	11	26	10	51.1	48.9
Indonesia	33	13	17	3	65.2	34.8

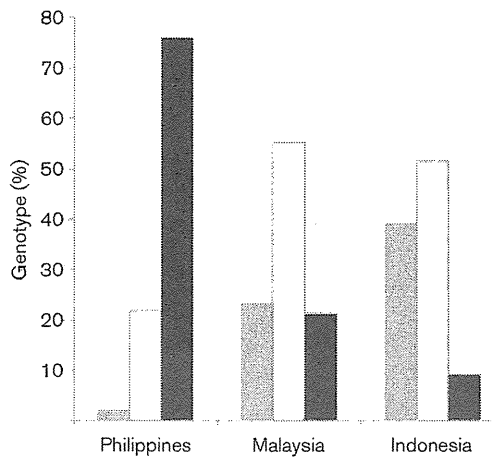


Fig. 2. Frequency of individuals having each *TRIM5* genotype. The percentages of *TRIM5α* homozygotes and heterozygotes and *TRIMCyp* homozygotes in each population were calculated. Grey bars, *TRIM5α* homozygote; white bars, heterozygote; black bars, *TRIMCyp* homozygote.

the N-terminal region, 44 (K→E) in the RING domain, 178 [H→tyrosine (Y)] and 209 (K→E) in the coiled-coil domain, and 247 (E→D) and 285 (G→R) in the linker domain (Fig. 3a). We found only one chromosome for minor allele 4G, two for 44E, four for 178Y, nine for 209E, five for 247D and four for 285R among 18 chromosomes from the six *TRIMCyp* homozygotes and three *TRIM5α* homozygotes. Among the six *TRIMCyp* homozygotes, we also found three E→Q substitutions at aa 296, which was present in *TRIMCyp* but absent from *TRIM5α*. There was no polymorphism that showed strong linkage disequilibrium with either the DK or NE haplotype except for G285R. The NE haplotype tended to link with 285G, although several DK haplotypes also linked with 285G (Supplementary Table S1). The numbers of polymorphic positions were relatively small among CMs compared with RMs (Fig. 3b). It is known that the coiled-coil region of *TRIM5* genes shows a high degree of genetic diversity in RMs (Johnson & Sawyer, 2009). In contrast, the coiled-coil

domain of CM *TRIM5α* and *TRIMCyp* showed no polymorphism at aa 184, 196, 208, 222, 230 and 236, which were all highly polymorphic in RMs (Newman *et al.*, 2006). These results suggest that the evolutionary pressures targeting the coiled-coil domain of the *TRIM5* gene were weaker in CMs than in RMs.

We also determined the nucleotide sequences of exon 8 encoding the PRYSPRY domain, of 12 *TRIM5α* homozygotes including the three *TRIM5α* homozygotes analysed above (see Supplementary Table S2, available in JGV Online). We found polymorphisms at aa 311 [serine (S)→leucine (L)], 327 (P→T), 330 [valine (V)→methionine (M)], 350 [V→isoleucine (I)] and 435 (I→V) in the PRYSPRY domain (Fig. 3a). Among the 12 *TRIM5α* homozygotes, we did not find a TFP allele at aa 339–341, which is a major determinant for different virus specificity between CM and RM *TRIM5αs* (Kono *et al.*, 2008) and is also critical for SIV from sooty mangabeys (SIVsm) (Kirmaier *et al.*, 2010) and SIVmac (Lim *et al.*, 2010) restriction by RM *TRIM5α*. We found only one chromosome for minor allele 311L, one for 327T, one for 350I and four for 435V among 11 *TRIM5α* homozygotes. We previously cloned CM *TRIM5α* cDNA from HSC-F cells (GenBank accession no. AB210052) (Nakayama *et al.*, 2005) and found that it contained 330V; however, all of the sequences determined in the present study showed M at this position. In contrast, exon 8 of the *TRIMCyp* gene of seven *TRIMCyp* homozygotes (all were heterozygotes for the DK and NE haplotypes), which encoded the PRYSPRY domain but was absent from the mRNA due to splicing, showed a uniform sequence identical to that of the Mamu 7 haplotype of RMs (307P, 313V, 327P, 332R, 333T, 334Q, 339Q, 345I, 383P, 414V, 420S and 488M). We only found one F→L substitution at position 454 among the seven *TRIMCyp* homozygotes. The Mamu 7 sequence is thus likely to be an ancient prototype sequence of *TRIMCyp* before the separation of CMs from RMs.

Anti-lentiviral activity of CM *TRIMCyps*

To elucidate the impact of CM *TRIMCyp* and its SNPs on the anti-lentiviral activity, we constructed a recombinant

Table 2. Frequencies of DK and NE haplotypes in CM *TRIMCyps*

Origin	No. of animals	Genotype (no. of chromosomes)				Frequency (%)	
		TRIM5α/TRIMCyp heterozygote*		TRIMCyp homozygote†		DK	NE
		DK	NE	DK	NE		
Philippines	28	6	1	36	6	85.7	14.3
Malaysia	21	14	1	10	2	88.9	11.1
Indonesia	15	12	0	4	2	88.9	11.1

*Haplotypes were determined by direct sequencing of the PCR products.

†Haplotypes were inferred by maximum-likelihood estimation using the results of direct sequencing of the PCR products.

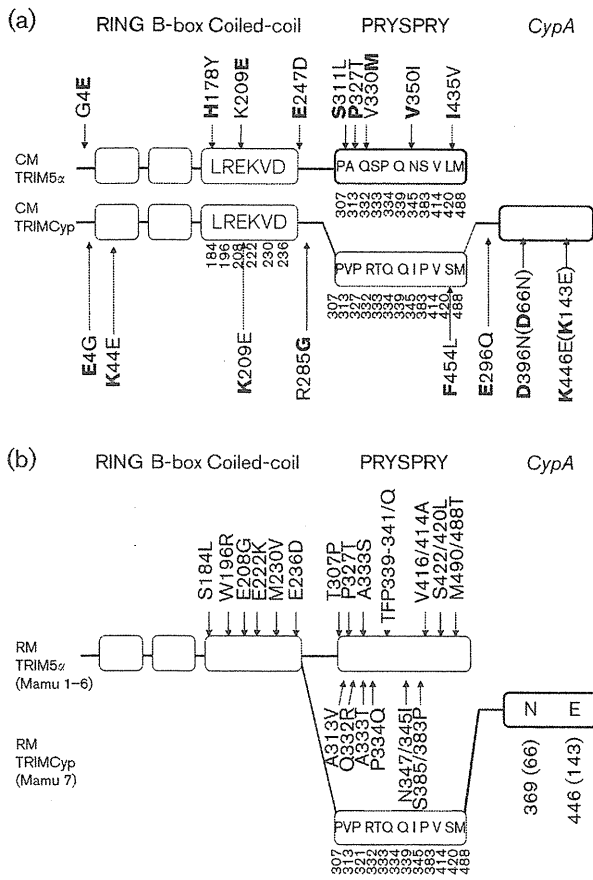


Fig. 3. Sequence variations in TRIM5 α and TRIMCyp. (a) Sequence variations in CM TRIM5 α and TRIMCyp. The RING, B-box, coiled-coil, PRYSPRY and CypA domains of CM TRIM5 α and TRIMCyp are indicated by open boxes. The box with thin lines shows exons 7 and 8 of the TRIMCyp gene, which is absent from the mRNA. Polymorphisms are shown outside the boxes, with downward and upward arrows indicating the polymorphisms observed among TRIM5 α homozygotes and TRIMCyp homozygotes, respectively. Amino acid residues found in HSC-F cells are shown in front of the amino acid positions, followed by the observed polymorphisms. Major alleles are shown in bold. Numbers in parentheses indicate amino acid positions counting from the initiation methionine codon of the CypA ORF. Amino acid residues in the boxes are polymorphic in the RM TRIM5 gene but lack polymorphism in CM TRIM5 α or TRIMCyp. Positions of these amino acid residues are shown below the boxes. (b) Sequence variations of RM TRIM5 α (Mamu 1–6) and TRIMCyp (Mamu 7). Downward and upward arrows indicate the polymorphisms observed in TRIM5 α and TRIMCyp, respectively. Amino acid residues in boxes indicate those of RM TRIMCyp. Positions of these amino acid residues are shown below the boxes.

Sendai virus (SeV) expressing a series of TRIM5 α /TRIMCyp: CM TRIM5 α , the DK and NE haplotypes of the CM TRIMCyp [CM TRIMCyp-major (DK) and CM TRIMCyp-minor (NE)], CM SPRY (–) in which the

PRYSPRY domain was deleted as a negative control for functional TRIM5 α and TRIMCyp, and an RM TRIMCyp. We also constructed a recombinant SeV expressing a CM TRIMCyp-minor (NE) carrying G at position 285 (CM TRIMCyp-minor R285G), as the NE haplotype seemed to be in linkage disequilibrium with G at this position (Supplementary Table S1). As shown in Fig. 4(a), upper panels], TRIMCyp-major (DK) completely restricted HIV-1 NL4-3, weakly restricted HIV-2 GH123 and failed to restrict SIVmac239. In contrast, TRIMCyp-minor (NE) and TRIMCyp-minor R285G inefficiently restricted HIV-1 NL4-3, barely restricted SIVmac239 and completely restricted HIV-2 GH123. These results indicated that the sequence variations in CM TRIMCyp greatly altered the spectrum of its anti-lentiviral activity. It should be noted that HIV-1 NL4-3 attained slightly higher titres at day 3 in cells expressing TRIMCyp-minor R285G than in those expressing TRIMCyp-minor (NE). The difference was small but reproducible in six independent experiments. This result indicated that aa 285 of TRIMCyp also affected its antiviral activity. In the case of RMs, in which the CypA domain of TRIMCyp has the same amino acid sequence as CM TRIMCyp-minor (NE), RM TRIMCyp showed the same spectrum of anti-lentiviral activity as CM TRIMCyp-minor (NE) (Fig. 4a, lower panels), consistent with previous reports (Price *et al.*, 2009; Wilson *et al.*, 2008a).

Finally, we examined whether HIV-1mt NL-DT5R (Kamada *et al.*, 2006) could evade restriction by CM TRIM5 α /TRIMCyp. HIV-1mt possesses core antigen (CA) with the SIVmac239-derived loop between α -helices 4 and 5 (L4/5), which corresponds to a CypA-binding loop of HIV-1, the entire SIVmac239 *vif* gene and two non-synonymous substitutions in the *env* gene (Fig. 4b). As shown in Fig. 4(c), NL-DT5R was restricted by TRIM5 α but completely evaded restriction by CM TRIMCyp-major (DK), suggesting that replacement of the CypA-binding loop of HIV-1 CA with the corresponding SIVmac239-derived sequence was sufficient to render HIV-1 resistant to the major haplotype of CM TRIMCyp but not TRIM5 α .

DISCUSSION

In the present study, we analysed the geographical, genetic and functional diversity of CM TRIMCyp and found: (i) a clear geographical deviation in the frequency of TRIMCyp, (ii) no typical geographical deviation in the frequency of the DK/NE haplotypes in the CypA domain, and (iii) sequence variations in the CypA domain of CM TRIMCyp, which greatly altered the spectrum of its anti-lentiviral activity.

We first demonstrated that the allele frequency of TRIMCyp in CMs from the Philippines was significantly higher than those in Indonesian and Malaysian CMs. It is possible that some pathogen(s) resistant to the antiviral effect of either TRIM5 α or TRIMCyp may contribute to this deviation as a selective pressure. As primate lentiviruses such as HIV-1 and

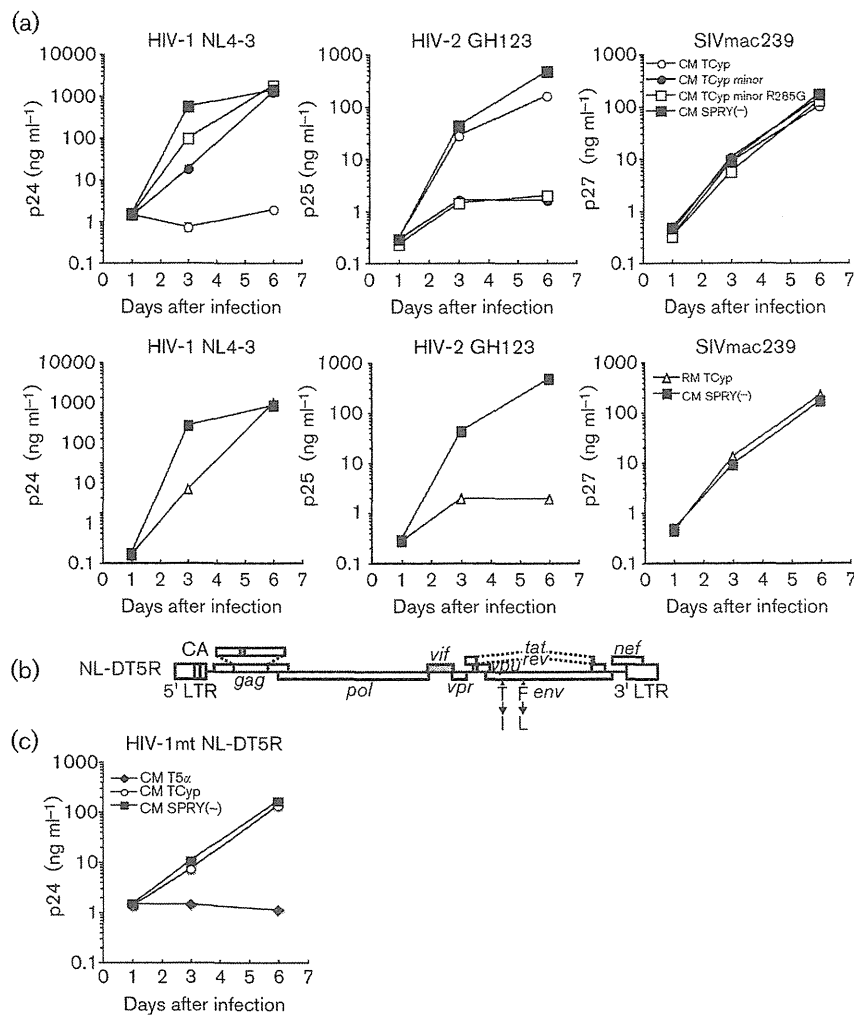


Fig. 4. Anti-lentiviral activity of various CM TRIMCyp. (a) MT4 cells were infected with recombinant SeV expressing CM TRIMCyp-major (DK) (CM TCyp; ○), CM TRIMCyp-minor (NE) (CM TCyp minor; ●), CM TRIMCyp-minor R285G (CM TCyp minor R285G; □), CM SPRY (-) (■) or RM TRIMCyp (RM TCyp; △). Data for CM SPRY (-) in the upper and lower panels were identical. Nine hours after infection, cells were superinfected with HIV-1 NL4-3, HIV-2 GH123 or SIVmac239. Culture supernatants were assayed separately for levels of p24, p25 or p27. (b) Structure of HIV-1mt NL-DT5R used in the experiment shown in Fig. 3(c). Open boxes denote HIV-1 (NL4-3) and shaded boxes denote SIVmac239 sequences. (c) MT4 cells were infected with recombinant SeV expressing CM TRIM5 α (CM T5 α ; ◆), CM TRIMCyp-major (DK) (CM TCyp; ○) or CM SPRY (-) (■). Nine hours after infection, cells were superinfected with HIV-1mt NL-DT5R. Culture supernatants were assayed separately for levels of p24. Error bars show actual fluctuations between duplicate samples. Data from a representative of three (a) or two (c) independent experiments are shown.

SIV originated in African primates, it is unlikely that these viruses could contribute directly to this deviation, and some exogenous and endogenous retroviruses may thus play a critical role in this selection. Alternatively, it is possible that this deviation could come from bottleneck effects. It is estimated that the Philippine CMs were derived from Indonesian CM stocks via sea rafting or terrestrial access through Borneo during periods of low sea level in South-East Asia around 110 000 years ago (Abegg & Thierry, 2002;

Blancher *et al.*, 2008; Kita *et al.*, 2009). Furthermore, phylogenetic analyses of mitochondrial DNA sequences of four CM populations distributed in South-East Asia suggested that Philippine CMs were derived from the small founding populations of Indonesian CMs, resulting in low genetic and nucleotide diversities (Blancher *et al.*, 2008). Importantly, however, as the Philippine CMs involved in this study at least originated from Luzon and Mindanao, the results in this study may reflect the frequency of TRIMCyp

in Philippine CMs as a whole, but do not represent local TRIMCyp distribution. In addition, hybridization with RMs may affect the prevalence of TRIMCyp. As Chinese RMs have been reported to have a low frequency of TRIMCyp (Newman *et al.*, 2008; Wilson *et al.*, 2008a), it is possible that interspecies mating with Chinese RMs might result in a lower prevalence of TRIMCyp in the Malaysian and Indonesian populations. In any case, it will be of great interest to determine the allele frequency of TRIMCyp in wild CMs to confirm whether our results reflect the observations in nature.

It is worth noting that the habitat of PMs is close to that of CMs, and in fact both species inhabit Indonesia; however, PMs reportedly express TRIMCyp but not TRIM5 α (Brennan *et al.*, 2008; Liao *et al.*, 2007). In contrast, the allele frequency of TRIMCyp in Indonesian CMs was shown to be markedly lower (Table 1). This discrepancy in frequency of TRIMCyp between PMs and CMs suggests that the two species have independently evolved antiretroviral factors to counteract some pathogen(s) existing in their habitats. It is possible that unidentified co-factors that interact with TRIM5 α /TRIMCyp may have a role in this discrepancy. Alternatively, the pathogen(s) could develop severe diseases in either monkey species. In the case of RMs, whilst the allele frequency of TRIMCyp was approximately 25% in the Indian population, TRIMCyp was not detected in the Chinese population (Wilson *et al.*, 2008a). Although the precise reason(s) for these geographical deviations in CMs and RMs is still unknown, it is reasonable to speculate that the possible pathogens, including exogenous and endogenous retroviruses, are/were heterogeneously disseminated, depending on their habitats.

The amino acid sequence of the CypA domain of our CM TRIMCyp-major (DK) is identical to that of Mafa TRIMCyp2 cloned by Ylinen *et al.* (2010); thus, CM TRIMCyp-major (DK) showed almost identical antiviral properties to those of Mafa TRIMCyp2. However, CM TRIMCyp-major (DK) slightly restricted HIV-2 GH123, although Mafa TRIMCyp2 failed to restrict HIV-2 ROD. This discrepancy is possibly due to differences in assays; Ylinen and co-workers performed a single-round infection assay using replication-incompetent virus, whereas we performed a multiple-round replication assay using replication-competent virus and thus our assay could detect weak restriction activities. It is also possible that differences in HIV-2 strains or TRIMCyp amino acid differences outside the CypA domain could affect the result.

In the case of CM TRIMCyp-minor (NE), the amino acid sequence of the CypA domain was identical to that of RM TRIMCyp, and antiviral properties of CM TRIMCyp-minor (NE) were the same as those of RM TRIMCyp. In addition, exon 8 of both TRIMCyp genes showed a uniform sequence, identical to that of the Mamu 7 haplotype of RMs. Exon 8 of TRIMCyp would have been free from selection pressures, as it is absent from the mRNA due to splicing, and the ancestral sequences in exon 8 would have been preserved. Taken together, it is reasonable to speculate that this minor

haplotype of CM TRIMCyp was the ancestor when CMs separated from RMs, and the major haplotype of CM TRIMCyp has arisen due to a specific evolutionary pressure on CMs. It should be noted that CM TRIM5 α has Q at aa 339, where RM TRIM5 α has a Q \rightarrow TFP polymorphism. This Q \rightarrow TFP polymorphism in the PRYSPRY domain also altered the spectrum of anti-lentiviral activity of TRIM5 α (Kirmaier *et al.*, 2010; Kono *et al.*, 2008; Lim *et al.*, 2010; Wilson *et al.*, 2008b). Therefore, it is tempting to speculate that the selection pressure in CMs drove amplification and diversification in TRIMCyp, whilst that in RMs drove diversification of the PRYSPRY domain of TRIM5 α .

In parallel with our study, Dietrich *et al.* (2011) recently reported the prevalence and functional diversity of TRIMCyp in CMs. They analysed populations from Indonesia, Indochina, Mauritius and the Philippines, and found that TRIMCyp was present in populations from Indonesia, Indochina and the Philippines, but not in populations from Mauritius. As they mentioned, the low genetic diversity, probably due to founder effects, may have led to the absence of TRIMCyp in the Mauritian population. In contrast, the small number of animals analysed may have resulted in the absence of TRIM5 α in their Philippine population. They also analysed the effects of DK \rightarrow NE substitution in CM TRIMCyp on antiretroviral activity by mutagenesis techniques. Furthermore, they found a unique individual with the DE haplotype in the CypA domain of TRIMCyp, whilst we did not identify such a haplotype in our study. Their results were essentially in accordance with ours, and we further demonstrated that Philippine CMs possessed TRIM5 α as well as TRIMCyp, suggesting that maintenance of both TRIM5 α and TRIMCyp in the CM population is beneficial to counteract challenges by retroviruses that are susceptible to TRIM5 α and by those susceptible to TRIMCyp. Consistent with this, Reynolds *et al.* (2011) demonstrated that heterozygotes of RMs with TRIM5 α and TRIMCyp showed higher resistance to repeated intrarectal challenge of SIVsmE660 compared with homozygotes for TRIM5 α or TRIMCyp. Interestingly, this different outcome was not observed in the case of intrarectal challenge with SIVmac239. As RM TRIMCyp restricts SIVsm but not SIVmac (Kirmaier *et al.*, 2010), the combination of TRIM5 α and TRIMCyp may function more efficiently as an antiviral factor against SIVsm.

We saw a small difference in anti-HIV-1 activity between CM TRIMCyp-minor (NE) and TRIMCyp-minor R285G. Dietrich *et al.* (2011) suggested that either of two polymorphic amino acid residues, K209E and R285G, might be responsible for attenuated anti-feline immunodeficiency virus activity of a certain haplotype of CM TRIMCyp. Our CM TRIMCyp-minor (NE) had K at aa 209, and an additional R285G mutation slightly attenuated the anti-HIV-1 activity of CM TRIMCyp-minor (NE). Residue 285 is in the linker region between the coiled-coil and CypA domains. The precise mechanism of how aa 285 affects anti-HIV-1 activity is unclear at present, but our result was consistent with those of Dietrich *et al.* (2011) and further revealed the importance of a single amino acid

substitution at aa 285 on the antiviral activity of CM TRIMCyp.

We showed that a prototypic HIV-1mt, named NL-DT5R, encoding L4/5 of SIVmac239 CA instead of that derived from HIV-1, evaded restriction by the major haplotype of CM TRIMCyp. As only HIV-1-derived L4/5 but not the SIVmac-derived L4/5 is expected to bind to CypA (Franke *et al.*, 1994), the substitution of L4/5 results in loss of binding of the capsid from CypA as well as TRIMCyp. Moreover, we recently demonstrated that HIV-1mt has the ability to grow in CMs (Saito *et al.*, 2011). Retrospective analysis of the TRIM5 genotypes of the infected CMs revealed that they were homozygous for TRIMCyp (data not shown), suggesting that TRIMCyp homozygotes allow the replication of HIV-1mt *in vivo*. These findings will be helpful not only to understand the molecular mechanisms of the species barrier of primates to lentiviruses, but also to emphasize the importance of TRIM5 genotypes for future studies regarding non-human primate models for HIV-1 infection.

METHODS

Sample collection. Blood samples were obtained from CMs kept in the Tsukuba Primate Research Center (TPRC), National Institute of Biomedical Innovation, Tsukuba, Japan. CMs have been maintained in indoor facilities as closed colony monkeys in TPRC since 1978 (Honjo, 1985). CMs in TPRC were obtained from Indonesia, Malaysia and the Philippines. Although the detailed local information of their origin is unclear, more than 100 animals were introduced to each colony by dividing it several times. Basically, the monkeys have been bred as pure blood of each origin without interbreed crossing. The generation number of animals involved in this study ranged from two to four when we consider the wild-caught founders (introduced monkeys) as zero. These animals were maintained according to the rules of the National Institute of Biomedical Innovation and guidelines for experimental animal welfare. Bleeding was performed under ketamine hydrochloride anaesthesia.

PCR amplification and sequence analysis. Genomic DNA was extracted from peripheral blood mononuclear cells (PBMCs) of 126 CMs using a QIAamp DNA Blood Mini kit (Qiagen). To test for the CypA insertion, the 3' region of the TRIM5 gene was amplified by PCR using LA Taq (TaKaRa) with primers TC forward (5'-TGACTCTGTGCTCACCAAGCTCTTG-3') and TC reverse (5'-ACCCTACTATGCAATAAAACATTAG-3'), as described by Wilson *et al.* (2008a). The amplified products of CypA from 30 TRIMCyp homozygotes and 32 TRIMCyp/TRIM5 α heterozygotes were gel-purified and subjected to direct sequencing using the forward and reverse primers.

To determine the sequences of the RING, B-box, coiled-coil and linker domains of TRIM5 α and TRIMCyp, which span >15 kb of genomic DNA, we prepared phytohaemagglutinin (PHA)-stimulated PBMCs from six TRIMCyp homozygotes and three TRIM5 α homozygotes. Total RNA was extracted from these cells using TRIzol (Invitrogen), and the RNA was reverse-transcribed using SuperScript III reverse transcriptase (Invitrogen) with TC reverse primer for TRIMCyp or TRIM5 reverse primer (5'-GAATTCTCAAGAGCTGGTGA-3') for TRIM5 α . The resultant cDNA was then PCR-amplified with LA Taq and forward primer TRIM5-235F (5'-GCAGGACCAGTGGAAATAGC-3'). The amplified products were purified and subjected to direct sequencing using primers TRIM5-235F, TRIM-N (5'-AGGCAGAAGCAGCAGGAA-3'), TRIM-Nrev

(5'-TTCCTGCTGCTTCTGCCT-3') and TRIM-E (5'-ACCTCCCAGTAATGTTC-3'). As the direct sequencing results of exons 5 and 6 of TRIMCyp were ambiguous because of the existence of the other splicing variant containing exons 1–4 combined with CypA (Brennan *et al.*, 2008), amplified products were then cloned into the vector pCR-2.1TOPO (Invitrogen) and the nucleotide sequences of numerous independent clones (between three and nine) for each TRIMCyp were determined.

Exon 8 (PRYSPRY domain) was PCR-amplified from 12 TRIM5 α homozygotes and seven TRIMCyp homozygotes by using TRIM-genotyping forward (5'-CTTCTGAACAAGTTTCTCCCAG-3') and reverse (5'-ATGAGATGCACATGGACAAGAGG-3') primers. The amplified products were purified and subjected to direct sequencing using the TRIM genotyping forward and reverse primers.

Cloning and expression of TRIMCyp. cDNA of the major haplotype of CM TRIMCyp, CM TRIMCyp-major (DK), was amplified by RT-PCR of mRNA extracted from the TRIM5 α /TRIMCyp-heterozygous CM T-cell line HSC-F using Not7TRIM5 (5'-GCCGCCGAGCTACTATGGCTTCTG-3') as the forward primer (NotI site underlined) and CypA Rev (5'-ACGGCGGTCTTTTCATTTCGAGTTGTCC-3') as the reverse primer. RM TRIMCyp cDNA was amplified by RT-PCR of mRNA extracted from the TRIMCyp homozygous RM T-cell line HSR5.4 using Not7TRIM5 as the forward primer and CypA Rev as the reverse primer. The amplified products were then cloned into pCR-2.1TOPO and the authenticity of the nucleotide sequence was verified. To generate TRIMCyp cDNAs carrying a haemagglutinin (HA; YPYDVPDYAA) tag at the C terminus, the TRIMCyp cDNA clones were used as templates for PCR amplification with a primer including a NotI site and an HA tag.

To generate the minor haplotype, CM TRIMCyp-minor (NE), the C-terminal portion of RM TRIMCyp (*SalI*-*NotI*) and the N-terminal portion of CM TRIMCyp-major (DK) (*NotI*-*SalI*) were assembled in the pcDNA3.1 (-) vector (Invitrogen). CM TRIMCyp-minor R285G was generated by site-directed mutagenesis by a PCR-mediated overlap primer-extension method.

The entire coding sequences of these TRIMCyps were then transferred to the *NotI* site of the pSeV18+b (+) vector. Recombinant SeVs carrying various TRIMCyp were recovered according to a previously described method (Nakayama *et al.*, 2005). The viruses were passaged twice in embryonated chicken eggs and used as stocks for all experiments.

Virus propagation. Virus stocks were prepared by transfection of 293T cells with HIV-1 NL4-3, HIV-2 GH123, SIVmac239 and HIV-1mt NL-DT5R (Kamada *et al.*, 2006) using a calcium phosphate coprecipitation method. Virus titres were measured using p24 (for HIV-1 and HIV-1mt) or p27 (for HIV-2 and SIVmac239) RetroTek antigen ELISA kits (ZeptoMetrix).

Virus infection. Aliquots of 2×10^5 MT4 cells were infected with SeV expressing CM TRIM5 α or each TRIMCyp at an m.o.i. of 10 and incubated at 37 °C for 9 h. Cells were then superinfected with 20 ng HIV-1 NL4-3 or HIV-1mt DT5R p24, 20 ng HIV-2 GH123 p25 or 20 ng SIVmac239 p27. The culture supernatants were collected periodically, and the levels of p24, p25 and p27 were measured with a RetroTek antigen ELISA kit.

ACKNOWLEDGEMENTS

The authors wish to thank Tomoko Ikoma, Setsuko Bandou and Noriko Teramoto for their helpful assistance. This work was supported by grants from the Ministry of Education, Culture,

Sports, Science, and Technology, the Ministry of Health, Labor, and Welfare in Japan, Global COE Program A06 of Kyoto University and Environment Research and Technology Development Fund (D-1007) of the Ministry of the Environment, Japan.

REFERENCES

- Abe, G. & Thierry, B. (2002). Macaque evolution and dispersal in insular south-east Asia. *Biol J Linn Soc Lond* **75**, 555–576.
- Agy, M. B., Frumkin, L. R., Corey, L., Coombs, R. W., Wolinsky, S. M., Koehler, J., Morton, W. R. & Katze, M. G. (1992). Infection of *Macaca nemestrina* by human immunodeficiency virus type-1. *Science* **257**, 103–106.
- Blancher, A., Bonhomme, M., Crouau-Roy, B., Terao, K., Kitano, T. & Saitou, N. (2008). Mitochondrial DNA sequence phylogeny of 4 populations of the widely distributed cynomolgus macaque (*Macaca fascicularis fascicularis*). *J Hered* **99**, 254–264.
- Brennan, G., Kozyrev, Y. & Hu, S.-L. (2008). TRIMCyp expression in Old World primates *Macaca nemestrina* and *Macaca fascicularis*. *Proc Natl Acad Sci U S A* **105**, 3569–3574.
- Dietrich, E. A., Brennan, G., Ferguson, B., Wiseman, R. W., O'Connor, D. & Hu, S.-L. (2011). Variable prevalence and functional diversity of the antiretroviral restriction factor TRIMCyp in *Macaca fascicularis*. *J Virol* **85**, 9956–9963.
- Franke, E. K., Yuan, H. E. & Luban, J. (1994). Specific incorporation of cyclophilin A into HIV-1 virions. *Nature* **372**, 359–362.
- Honjo, S. (1985). The Japanese Tsukuba Primate Center for Medical Science (TPC): an outline. *J Med Primatol* **14**, 75–89.
- Johnson, W. E. & Sawyer, S. L. (2009). Molecular evolution of the antiretroviral TRIM5 gene. *Immunogenetics* **61**, 163–176.
- Kamada, K., Igarashi, T., Martin, M. A., Khamsri, B., Hatcho, K., Yamashita, T., Fujita, M., Uchiyama, T. & Adachi, A. (2006). Generation of HIV-1 derivatives that productively infect macaque monkey lymphoid cells. *Proc Natl Acad Sci U S A* **103**, 16959–16964.
- Kirmaier, A., Wu, F., Newman, R. M., Hall, L. R., Morgan, J. S., O'Connor, S., Marx, P. A., Meythaler, M., Goldstein, S. & other authors (2010). TRIM5 suppresses cross-species transmission of a primate immunodeficiency virus and selects for emergence of resistant variants in the new species. *PLoS Biol* **8**, e1000462.
- Kita, Y. F., Hosomichi, K., Kohara, S., Itoh, Y., Ogasawara, K., Tsuchiya, H., Torii, R., Inoko, H., Blancher, A. & other authors (2009). MHC class I A loci polymorphism and diversity in three Southeast Asian populations of cynomolgus macaque. *Immunogenetics* **61**, 635–648.
- Kono, K., Song, H., Shingai, Y., Shioda, T. & Nakayama, E. E. (2008). Comparison of anti-viral activity of rhesus monkey and cynomolgus monkey TRIM5s against human immunodeficiency virus type 2 infection. *Virology* **373**, 447–456.
- Liao, C.-H., Kuang, Y.-Q., Liu, H.-L., Zheng, Y.-T. & Su, B. (2007). A novel fusion gene, TRIM5-Cyclophilin A in the pig-tailed macaque determines its susceptibility to HIV-1 infection. *AIDS* **21** (Suppl. 8), S19–S26.
- Lim, S.-Y., Rogers, T., Chan, T., Whitney, J. B., Kim, J., Sodroski, J. & Letvin, N. L. (2010). TRIM5 α modulates immunodeficiency virus control in rhesus monkeys. *PLoS Pathog* **6**, e1000738.
- Nakayama, E. E. & Shioda, T. (2010). Anti-retroviral activity of TRIM5 α . *Rev Med Virol* **20**, 77–92.
- Nakayama, E. E., Miyoshi, H., Nagai, Y. & Shioda, T. (2005). A specific region of 37 amino acid residues in the SPRY (B30.2) domain of African green monkey TRIM5 α determines species-specific restriction of simian immunodeficiency virus SIVmac infection. *J Virol* **79**, 8870–8877.
- Newman, R. M., Hall, L., Connole, M., Chen, G.-L., Sato, S., Yuste, E., Diehl, W., Hunter, E., Kaur, A. & other authors (2006). Balancing selection and the evolution of functional polymorphism in Old World monkey TRIM5 α . *Proc Natl Acad Sci U S A* **103**, 19134–19139.
- Newman, R. M., Hall, L., Kirmaier, A., Pozzi, L. A., Pery, E., Farzan, M., O'Neil, S. P. & Johnson, W. (2008). Evolution of a TRIM5-CypA splice isoform in Old World monkeys. *PLoS Pathog* **4**, e1000003.
- Nomaguchi, M., Doi, N., Kamada, K. & Adachi, A. (2008). Species barrier of HIV-1 and its jumping by virus engineering. *Rev Med Virol* **18**, 261–275.
- Price, A. J., Marzetta, F., Lammers, M., Ylinen, L. M., Schaller, T., Wilson, S. J., Towers, G. J. & James, L. C. (2009). Active site remodeling switches HIV specificity of antiretroviral TRIMCyp. *Nat Struct Mol Biol* **16**, 1036–1042.
- Reynolds, M. R., Sacha, J. B., Weiler, A. M., Borchardt, G. J., Glidden, C. E., Sheppard, N. C., Norante, F. A., Castrovinci, P. A., Harris, J. J. & other authors (2011). The TRIM5 α genotype of rhesus macaques affects acquisition of simian immunodeficiency virus SIVsmE660 infection after repeated limiting-dose intrarectal challenge. *J Virol* **85**, 9637–9640.
- Saito, A., Nomaguchi, M., Iijima, S., Kuroishi, A., Yoshida, T., Lee, Y.-J., Hayakawa, T., Kono, K., Nakayama, E. E. & other authors (2011). Improved capacity of a monkey-tropic HIV-1 derivative to replicate in cynomolgus monkeys with minimal modifications. *Microbes Infect* **13**, 58–64.
- Sauter, D., Specht, A. & Kirchhoff, F. (2010). Tetherin: holding on and letting go. *Cell* **141**, 392–398.
- Song, H., Nakayama, E. E., Yokoyama, M., Sato, H., Levy, J. A. & Shioda, T. (2007). A single amino acid of the human immunodeficiency virus type 2 capsid affects its replication in the presence of cynomolgus monkey and human TRIM5s. *J Virol* **81**, 7280–7285.
- Stremelau, M., Owens, C. M., Perron, M. J., Kiessling, M., Autissier, P. & Sodroski, J. (2004). The cytoplasmic body component TRIM5 α restricts HIV-1 infection in Old World monkeys. *Nature* **427**, 848–853.
- Wilson, S. J., Webb, B. L., Ylinen, L. M., Verschoor, E., Heeney, J. L. & Towers, G. J. (2008a). Independent evolution of an antiviral TRIMCyp in rhesus macaques. *Proc Natl Acad Sci U S A* **105**, 3557–3562.
- Wilson, S. J., Webb, B. L., Mplanka, C., Newman, R. M., Verschoor, E. J., Heeney, J. L. & Towers, G. J. (2008b). Rhesus macaque TRIM5 alleles have divergent antiretroviral specificities. *J Virol* **82**, 7243–7247.
- Yap, M. W., Nisole, S., Lynch, C. & Stoye, J. P. (2004). Trim5 α protein restricts both HIV-1 and murine leukemia virus. *Proc Natl Acad Sci U S A* **101**, 10786–10791.
- Ylinen, L. M., Price, A. J., Rasaiyaah, J., Hué, S., Rose, N. J., Marzetta, F., James, L. C. & Towers, G. J. (2010). Conformational adaptation of Asian macaque TRIMCyp directs lineage specific antiviral activity. *PLoS Pathog* **6**, e1001062.

RESEARCH

Open Access

Whole-genome sequencing and analysis of the Malaysian cynomolgus macaque (*Macaca fascicularis*) genome

Atsunori Higashino^{1,2}, Ryuichi Sakate^{1*}, Yosuke Kameoka¹, Ichiro Takahashi¹, Makoto Hirata¹, Reiko Tanuma¹, Tohru Masui¹, Yasuhiro Yasutomi³ and Naoki Osada^{4,5*}

Abstract

Background: The genetic background of the cynomolgus macaque (*Macaca fascicularis*) is made complex by the high genetic diversity, population structure, and gene introgression from the closely related rhesus macaque (*Macaca mulatta*). Herein we report the whole-genome sequence of a Malaysian cynomolgus macaque male with more than 40-fold coverage, which was determined using a resequencing method based on the Indian rhesus macaque genome.

Results: We identified approximately 9.7 million single nucleotide variants (SNVs) between the Malaysian cynomolgus and the Indian rhesus macaque genomes. Compared with humans, a smaller nonsynonymous/synonymous SNV ratio in the cynomolgus macaque suggests more effective removal of slightly deleterious mutations. Comparison of two cynomolgus (Malaysian and Vietnamese) and two rhesus (Indian and Chinese) macaque genomes, including previously published macaque genomes, suggests that Indochinese cynomolgus macaques have been more affected by gene introgression from rhesus macaques. We further identified 60 nonsynonymous SNVs that completely differentiated the cynomolgus and rhesus macaque genomes, and that could be important candidate variants for determining species-specific responses to drugs and pathogens. The demographic inference using the genome sequence data revealed that Malaysian cynomolgus macaques have experienced at least three population bottlenecks.

Conclusions: This list of whole-genome SNVs will be useful for many future applications, such as an array-based genotyping system for macaque individuals. High-quality whole-genome sequencing of the cynomolgus macaque genome may aid studies on finding genetic differences that are responsible for phenotypic diversity in macaques and may help control genetic backgrounds among individuals.

Background

Cynomolgus macaque (*Macaca fascicularis*) is one of the most commonly used nonhuman primates in biomedical research worldwide [1]. It is also called the crab-eating or long-tailed macaque and belongs to the *fascicularis* group of the genus *Macaca* [2]. A number of pharmaceutical companies use cynomolgus macaques for drug

development and, thus, identifying genetic components that contribute to their drug metabolism is a key issue in biomedical genomic research [3,4].

Rhesus macaque (*Macaca mulatta*), whose draft genome sequence was determined by the Sanger sequencing method with a BAC clone assembly [5], is genetically closely related to the cynomolgus macaque. Whereas rhesus macaques occur from India to southern China and in some neighboring areas, cynomolgus macaques can be found throughout Southeast Asia. Vital hybrids of the two macaques have been observed around northern Thailand, supporting their very close genetic relationship [6]. Previous studies have shown that cynomolgus and rhesus macaques share a considerable number of single

* Correspondence: rsakate@nibio.go.jp; nosada@nig.ac.jp

¹Laboratory of Rare Disease Biospecimen, Department of Disease Bioresources Research, National Institute of Biomedical Innovation, 7-6-8 Saito-asagi, Ibaraki, Osaka 567-0085, Japan

⁴Division of Evolutionary Genetics, Department of Population Genetics, National Institute of Genetics, 1111 Yata, Mishima, Shizuoka 411-8540, Japan
Full list of author information is available at the end of the article

nucleotide variants (SNVs) [7,8]. Their genetic divergence is estimated to be approximately 0.4% [8,9].

Recently, several genome sequences of macaques have been determined using next-generation sequencing platforms. These include Mauritian and Vietnamese cynomolgus macaques [4,10], two independent Chinese rhesus macaques [10,11] and one Indian rhesus macaque [12]. The two cynomolgus macaque individuals (Mauritian and Vietnamese), however, were derived from two genetically distinct populations that have experienced peculiar demographic histories. Previous studies have suggested that cynomolgus macaques are genetically clustered into Indonesian-Malaysian, Philippine, Indochinese, and Mauritian macaques [8,13]. Mauritian macaques have been known to show extremely low genetic diversity that is associated with their recent colonization [14], whereas Indochinese macaques have experienced a considerable amount of gene flow with rhesus macaques [15,16]. Therefore, the whole-genome sequencing of Indonesian-Malaysian cynomolgus macaques, which show the highest genetic diversity and, according to the fossil evidence, originate from a putative ancestral population [17], would provide significant insight into the genetic differentiation of cynomolgus and rhesus macaques at the species level.

Recent advances in DNA sequencing technologies have enabled rapid and economical determination of whole-genome sequences of organisms. Although *de novo* assemblies of large and complicated genomes, such as mammalian genomes, remain difficult, whole-genome resequencing has become a powerful method for identifying genetic variation within a biological species. Human genome variation is of particular interest for medical and evolutionary studies, and a dozen human genome sequences have thus far been determined using resequencing methods [18-24]. Whole-genome resequencing is not only efficient for identifying variations within a species, but also applicable to closely related species. Because the current methods of mapping short DNA sequence reads have been developed to amend relatively high sequencing errors in massively parallel sequencing, they are also expected to be useful for small sequence divergence. Thus, the strategy of resequencing species that are closely related to model organisms of known genome sequence may be an efficient and important method for detecting genomic diversity.

In this study, we determined and analyzed the Malaysian cynomolgus macaque genome sequence using the massively parallel sequencer SOLiD 3 Plus System (Life Technologies). The sequenced reads were mapped to the Indian rhesus macaque (reference) genome sequence with more than 40-fold coverage. A total of approximately 9.7 million SNVs and 1 million small (< 12 bp) indels and 60,000 large indels (44 to 732 bp) were identified. The

identified SNVs were compared with SNVs previously determined for other cynomolgus and rhesus macaque genomes. These SNVs have been deposited in the cynomolgus macaque genome resources database (QFbase [25]). High-quality resequencing of the cynomolgus macaque genome will facilitate further studies directed towards dissecting genetic differences that are responsible for phenotypic divergence among macaque species.

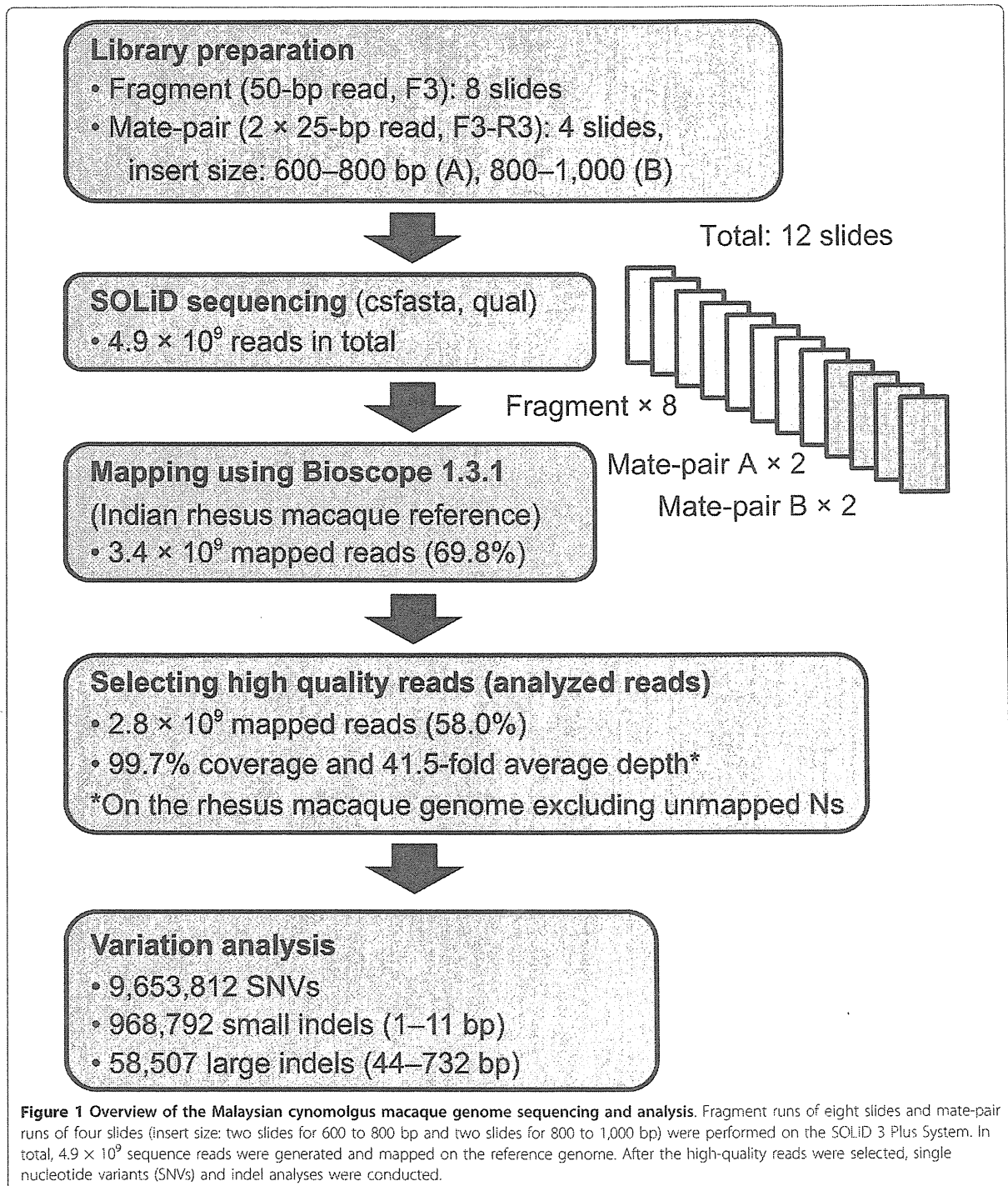
Results

Sequencing and mapping

Blood samples from a 25-year-old male Malaysian cynomolgus macaque were used for genome resequencing. Figure 1 outlines the procedure of the cynomolgus macaque genome resequencing. We performed eight cycles of fragment library sequencing (50 bp) and four cycles of mate-pair library sequencing (2×25 bp) using the SOLiD 3 Plus System. The mate-pair libraries of two different insert sizes (600 to 800 bp and 800 to 1,000 bp) were constructed and analyzed. Table 1 summarizes the results of genome sequencing and mapping. A total of 2.6×10^9 reads of fragment sequence and 2.2×10^9 reads of mate-pair sequence data were obtained. The mapping program implemented in BioScope software v1.3.1 (Life Technologies) was used for mapping the reads. A total of 3.4×10^9 reads (69.8%) were successfully mapped on the Golden Path genome assembly, which was derived from an Indian rhesus macaque (mmu_120505). Finally, analyzed reads totaled 1.1×10^{11} bp, and the average coverage depth was 41.5-fold. All chromosomes exceeded 37-fold (Figure S1 in Additional file 1). The analyzed reads covered 99.7% of the reference genome (unmapped Ns were excluded), and 95.8% of the reference genome was covered by at least 10 reads (Figure S2 in Additional file 1). In order to examine whether our mapping statistics depended on the genome assembly, we also mapped our reads to the recently determined Vietnamese cynomolgus macaque genome, which was constructed by *de novo* assembly of short reads [10]. As a result, a similar mapping rate level (67.2%) and genome coverage (42.5-fold) were obtained (Table S1 in Additional file 1). We primarily focus on the results obtained using the Golden Path genome assembly throughout the rest of the paper because the reference genome had more detailed genome annotations, and the results are comparable with those of other studies. Hereafter, we refer to the Golden Path genome assembly as the "reference" genome.

Single nucleotide variant detection

SNVs were called with SAMtools [26] using the mapped reads on the reference genome. SNVs at low (< 5) coverage sites and with low call quality values (QV < 40) were excluded. Because the reference genome sequence has



not yet been finalized, we examined the relationship between the quality of the reference genome assembly and the SNV discovery rate. We expected that homozygous SNVs in low-quality genomic regions were possible errors in the reference genome sequence and that

heterozygous SNVs were robust in genome quality. As shown in Figure 2, we plotted the proportions of homozygous and heterozygous SNVs against the reference genome QVs. Although the heterozygous SNV discovery rate was nearly constant across genome quality, homozygous

Table 1 Summary of SOLiD libraries and sequence reads

Library	Read length (bp)	Insert size (bp)	Runs	Reads	Mapped reads	Analyzed reads ^a	Coverage depth of analyzed reads
Fragment	50	-	8	2,648,128,521	1,976,720,560 (74.7%)	1,974,496,337 (74.6%)	33.4
Mate-pair A	25 (x2)	600-800	2	906,783,481	621,175,871 (68.5%)	355,589,008 _b (39.2%)	3.4
Mate-pair B	25 (x2)	800-1,000	2	1,335,583,547	814,866,634 (61.0%)	508,168,736 _b (38.0%)	4.8
Total	-	-	12	4,890,495,549	3,412,763,065 (69.8%)	2,838,254,081 (58.0%)	41.5

^aReads mapped on chrM and chrUr were removed. ^bPCR or optical duplicates (defined by Bioscope; mapped more than 100 loci) were removed, and properly paired reads were selected; each read of a pair was mapped on the same chromosome in a proper direction at a proper distance from each other.

SNV rates in low-quality regions were relatively high, suggesting that those SNVs were probably due to errors in the genome sequence and should be filtered out. In addition, we observed a slight peak in homozygous SNV rates at QV around 40. This pattern was also observed when we removed SNVs within repeat regions (data not shown) and may have been due to unknown problems in the assembly process of the reference genome sequence. Based on this observation, we decided to filter out SNVs at sites having QVs < 45 in the reference genome sequence. This filtering did not significantly sacrifice our SNV detection power, because > 94% of the reference rhesus macaque genome had QV = 60.

Using the above criteria, we identified 4,880,874 heterozygous and 4,527,169 homozygous SNVs on autosomes. The number of estimated SNVs is summarized in Table 2. Note that the numbers in this table are underestimates because SNVs ambiguously assigned as either homozygous or heterozygous were not included (see Materials and methods). In autosomal non-coding regions, 42,930 untranslated exonic (5'/3' UTR), 2,878,903 intronic, and

6,422,898 intergenic SNVs were identified. Among them, 3,707,670 SNVs were mapped to repeat regions. The nucleotide change pattern of the SNVs is shown in Table S2 in Additional file 1. The transition-to-transversion ratio was 2.39, which is close to the estimated value in humans [27]. SNV densities on chromosomes are summarized in Figure S3 in Additional file 1. Using the same SNV-detecting criteria, we identified about 8.5 million SNVs by mapping Malaysian cynomolgus macaque reads on the Vietnamese cynomolgus macaque genome sequences.

Among 18,912 annotated autosomal protein-coding genes, 14,560 carried at least one coding SNV, consisting of 25,079 nonsynonymous and 38,233 synonymous SNVs. We found that 9,753 autosomal genes contained at least one heterozygous or homozygous amino acid variation in the Malaysian cynomolgus macaque genome, compared with the reference rhesus macaque genome. In addition, 108 and 200 autosomal genes harbored non-sense mutations that were homozygous and heterozygous, respectively. We also estimated the number of SNVs on the X chromosome. Only homozygous SNVs on the X chromosome were counted. In total, we identified 245,769 SNVs on the X chromosome, including 1,145 coding (444 nonsynonymous and 701 synonymous SNVs in 662 protein-coding genes), 986 UTR, 50,877 intronic, and 192,761 intergenic homozygous SNVs (Table 2).

Comparisons with previously determined macaque genomes

The newly identified whole-genome SNVs between Malaysian cynomolgus and Indian (reference) rhesus macaques were compared with previously identified SNVs. We downloaded short-read sequences of Vietnamese cynomolgus and Chinese rhesus macaques that had comparable coverage depth to ours (> 40-fold) and mapped on the reference genome [10]. Using the same SNV-detecting pipeline, we identified 13,244,140 and 10,662,418 SNVs in the Vietnamese cynomolgus and Chinese rhesus macaque genomes, respectively. The Malaysian cynomolgus macaque shared 5,181,509 SNVs

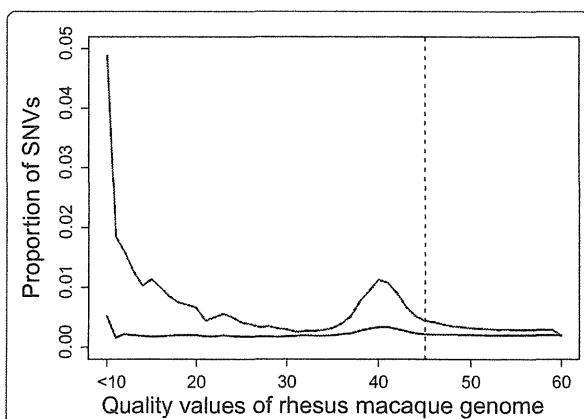


Figure 2 SNV discovery rate and rhesus macaque genome quality. The red and blue lines represent the rates of homozygous and heterozygous SNVs, respectively, with given rhesus macaque genome sequence quality values (QVs). SNVs at sites having QV < 45 (left of the dashed line) were filtered out.

Table 2 Number of single nucleotide variants

Chromosome	Heterozygous SNVs	Homozygous SNVs	A ^a	S ^b	UTR ^c	Intronic	Intergenic
Autosomes	4,880,874	4,527,169	25,079	38,233	42,930	2,878,903	6,422,898
X chromosomes	. ^d	245,769	444	701	986	50,877	192,761
Total	4,880,874	4,772,938	25,523	38,934	43,916	2,928,970	6,615,659

^aNumber of nonsynonymous SNVs. ^bNumber of synonymous SNVs. ^cNumber of SNVs in untranslated regions. ^dOnly homozygous SNVs were considered on the X chromosome.

with the Vietnamese cynomolgus macaque, either homozygous or heterozygous, showing that > 50% of our SNVs were shared between the two cynomolgus macaque individuals. Merging the two cynomolgus macaque genomes yielded 17,716,443 SNVs in cynomolgus macaques. Furthermore, we found that 2,519,988 SNVs were restricted to the Malaysian cynomolgus macaque, and 1,368,528 SNVs were completely differentiated between the two cynomolgus and two rhesus macaque genomes. Because sequencing platforms and coverage depth differed among the studies, we could not directly compare the number of inferred SNVs. We therefore compared the fraction of heterozygous SNVs shared between two genomes. About 8% of Malaysian and 11% of Vietnamese heterozygous SNVs were also heterozygous SNVs in the Chinese rhesus macaque, supporting the contention that Indochinese cynomolgus macaques have been more vulnerable to gene introgression from rhesus macaques than Indonesian-Malaysian macaques.

We next searched for immune- and drug-response genes that carried nonsynonymous SNVs in the Malaysian cynomolgus macaque, because these genes are of particular interest in biomedical research. In total, 72 and 42 autosomal genes, of which the human orthologs had been annotated as immune-response (GO: 0006955) and drug-response (GO: 0042493) genes, respectively, had at least one homozygous amino acid change in the Malaysian cynomolgus macaque genome. We further checked whether these homozygous SNVs were likely to be differentiated between the two macaque species. A handful of genes, 29 immune- and 18 drug-response genes, carried completely segregating nonsynonymous SNVs between cynomolgus and rhesus macaques, for a total of 60 nonsynonymous SNVs (Table S3 in Additional file 1).

Population genetic inferences from resequenced data

In contrast to previous resequencing studies, the reference genome and the resequenced genome in this study were from highly differentiated but not completely isolated populations. The average genetic diversity in cynomolgus macaques (nucleotide diversity) corresponded to the fraction of heterozygous SNVs (differences between two sequenced chromosomes) if there was no consanguinity effect, whereas the average genetic divergence

between species (Nei's d_{xy}) [28] corresponded to the fraction of homozygous SNVs plus one-half of the heterozygous SNVs.

In order to infer the strength of natural selection within and between macaque species, we estimated the ratio of nonsynonymous to synonymous SNVs. The ratio of nonsynonymous to synonymous heterozygous SNVs within cynomolgus macaques was 0.68. In order to compare the ratios in macaques and humans, a diploid human genome sequence determined by a short-read sequencer with similar read depth (African genome, NA19839) was retrieved from the public database. The human SNVs were determined using the same SNV-detecting pipeline described above. The ratio of nonsynonymous to synonymous heterozygous SNVs in the African human genome was 0.89, significantly higher than the ratio in the macaque ($P < 10^{-15}$, chi-square test). This pattern agrees well with the nearly neutral theory, in which slightly deleterious mutations tend to be segregated within small populations [29], because these macaques have four to five times larger effective population sizes than extant humans. In addition, the ratio within cynomolgus macaques (0.68) was slightly but statistically and significantly higher than that between cynomolgus and rhesus macaques (0.65; $P = 0.002$, chi-square test). If most of the nonsynonymous SNVs between cynomolgus and rhesus macaques were due to diversifying selection between species, the ratio of nonsynonymous to synonymous SNVs between species should be higher than that within species. This pattern also could be explained by the nearly neutral theory, wherein slightly deleterious mutations are short-lived and cannot contribute to species differentiation.

Small indels detected by sequence mapping

Using the mapping information of sequence reads, we also estimated the number of small indels (< 12 bp) in the Malaysian cynomolgus macaque genome. Interestingly, we observed a slight increase in small indels around QV = 40 of the reference genome sequence (Figure S4 in Additional file 1). We therefore filtered out small indels at sites with QV < 45 in the reference sequence. In total, we identified 365,581 insertions and 587,456 deletions on autosomes and 7,023 insertions and 8,732 deletions on the X chromosome. Only

homozygous indels were counted on the X chromosome. Out of 372,604 small insertions and 596,188 small deletions in total, 154,649 (42%) and 250,398 (42%) were assigned to repeat regions, respectively. Among 1,139 indels within autosomal protein-coding regions, 705 were frameshifting and 434 were non-frameshifting (3x-bp-length) indels. The proportion of 3x-bp-length indels (38%) was significantly higher than the value expected from intergenic indels (14%; $P < 10^{-15}$, chi-square test), suggesting purifying selection on frameshifting indels in coding regions. The distribution of small indel lengths is shown in Figure 3.

Large indels detected by mate-pair distance

An early chromosome-banding study suggested a paracentric chromosomal inversion in the long arm of chromosome 5 between cynomolgus and rhesus macaques [30]. In order to examine the occurrence of inversion at the chromosome-banding level (> 1 Mb), we surveyed mate-pair sequence reads that were not properly aligned

on chromosome 5. The number of mate-pair reads showing the signature of inversion was counted within 500-bp-length windows with 250-bp sliding steps. In total, 28 windows that contained ≥ 50 incongruent reads were found. However, all of the windows included alpha satellite repeats and none showed evidence of the large inversion.

We further analyzed the pattern of large insertions and deletions using the information from the mate-pair libraries of different insert sizes (mate-pair library A, 600 to 800 bp; library B, 800 to 1,000 bp). A total of 29,009 and 50,945 indels were identified using libraries A and B, respectively. Merging these indels yielded 8,301 insertions and 50,206 deletions; the insertion and deletion size ranges were 77 to 732 bp and 44 to 601 bp, respectively. Although the reference genome assembly has consecutive indices for each chromosome, the assembled genome sequences were built from scaffolds and contigs connected with assembly gaps (stretches of Ns). Among the 50,206 deletions, 45,821 and 22,774 encompassed repeat sequences and ambiguous sequences, respectively. Similarly, among the 8,301 insertions, 7,886 and 1,729 were within repeat sequences and ambiguous sequences, respectively. The distributions of insertion and deletion lengths that were not associated with gaps are shown in Figure S5 in Additional file 1.

Inference of demography

Recently, Li and Durbin [31] developed a novel method for inferring the demography of species from single diploid genome data. The demography is inferred from a distribution of coalescence time between two haploid genomes. We applied this method to our Malaysian cynomolgus genome data, with a generation time of 6 years and a mutation rate per generation of 2.5×10^{-8} . Figure 4 shows the inferred demography of the cynomolgus macaque with bootstrap 95% confidence interval. Although the scaling parameters affect the estimation of time and population size scales, the result showed at least three population bottlenecks in the past. In agreement with the previous estimates, the cynomolgus macaque population size expanded more than several fold during a million-year period [8,10,32].

Database resource

The Malaysian cynomolgus macaque genome sequence reads have been deposited to public databases (DDBJ Sequence Read Archive: DRA000430), and identified SNVs have been registered to the *Macaca fascicularis* genome database (QFbase [25]), which was previously built by our research group. The database was constructed based on the reference genome sequence of the Indian rhesus macaque, and the annotation of cynomolgus macaques was implemented, including cDNA

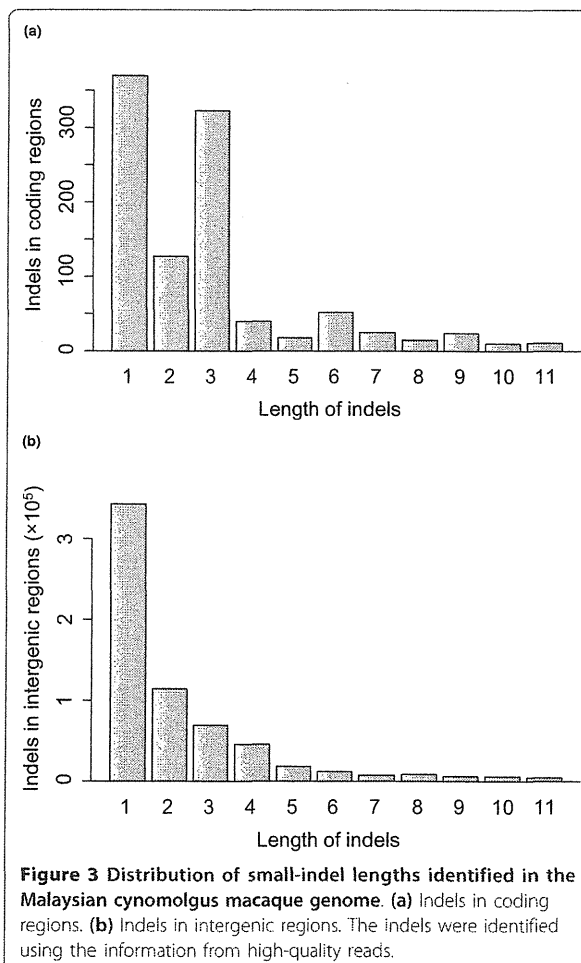
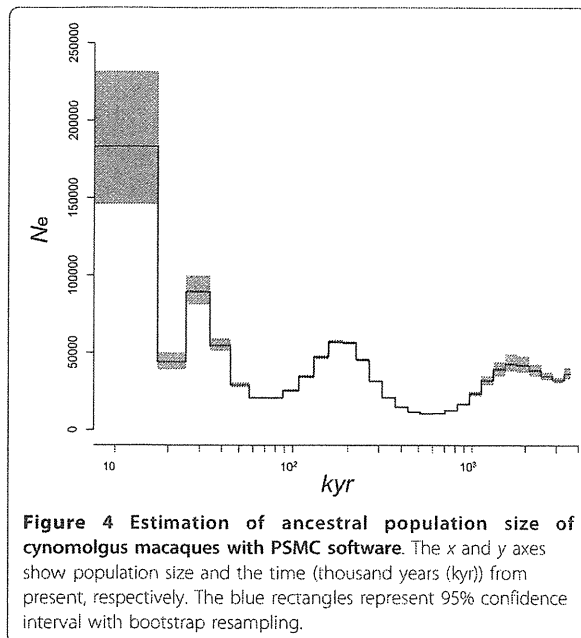


Figure 3 Distribution of small-indel lengths identified in the Malaysian cynomolgus macaque genome. (a) Indels in coding regions. (b) Indels in intergenic regions. The indels were identified using the information from high-quality reads.



sequences, BAC clones, and microsatellite markers [9,33]. An example of a graphical view of SNVs in the browser is shown in Figure 5. Because cynomolgus macaques are frequently used in animal experiments, these resources will be valuable for researchers who are not familiar with large-scale data manipulation.

Discussion

Controlling the genetic background of experimental animals is a key issue for the efficiency and reliability of pre-clinical trials in biomedical research. Previous studies have shown that macaques, which are the most popular primates for biomedical research, harbor much higher genetic diversity than humans, even if they are collected from a limited area [8,15,32]. Thus, high-quality whole-genome sequences of cynomolgus macaques are necessary for future biomedical studies in order to control and quantify differences in genetic backgrounds. In addition, many morphological and physiological differences have been reported between the macaque species, including behaviors, tail lengths, body sizes, and susceptibility to pathogens and drugs [34,35]. Determining genetic differences between cynomolgus and rhesus macaques that contribute to phenotypic differences between them is an important subject for both biomedical and evolutionary research.

In this study, we have identified about 9.7 million SNVs between Malaysian cynomolgus and Indian rhesus macaques and 8.5 million SNVs between Malaysian and Vietnamese cynomolgus macaques. The total number of SNVs is much higher than that estimated in human

genome resequencing studies (approximately 3 million). Although we cannot directly compare the number of SNVs determined with different platforms and different inference methods, the high level of genetic diversity within macaque species is in agreement with previous multi-locus sequencing studies using the Sanger method [8,32] and with the whole-genome sequencing study using a different platform with a similar level of genome coverage [10]. Despite the high level of genetic diversity within and between macaque species, the number of SNVs potentially responsible for species delimitation may be limited, partly owing to frequent gene flow between Indochinese cynomolgus and Chinese rhesus macaques. Only about 10% of SNVs were completely segregated between the two cynomolgus and two rhesus macaque genomes, which were further narrowed down to 60 nonsynonymous SNVs in drug- and immune-related genes.

The number of nonsynonymous SNVs was also higher in macaques than in humans. Whereas about 10,000 nonsynonymous SNVs were segregated in humans, about 30,000 nonsynonymous SNVs were segregated within and between macaque species. Interestingly, the level of protein diversity relative to background genetic diversity in macaques was significantly smaller than that expected from human data. This difference is probably due to the large effective population size of macaques, which removes slightly deleterious mutations in populations with relatively better efficiency.

Although we found a considerable number of SNVs and indels with high mapping support, we should be careful of some aspects of the quality of the reference genome assembly. In the large indel analysis using the mate-pair libraries, $\geq 90\%$ of large indels included repeat sequences in the genome, indicating that these are potential repeat regions for genome-size change. Unfortunately, because the data we obtained using the SOLiD platform are not suitable for *de novo* assembly of a whole-genome sequence, we cannot conclude whether or not these hotspots are due to artifacts stemming from the reference genome quality. *De novo* assembly of a whole mammalian genome sequence remains costly, but studies using multiple genomes with *de novo* assembly would elucidate the complex pattern of genome-size changes [10].

The demography of the Malaysian cynomolgus macaque reveals the complex history of macaque genomes. As geological and fossil evidence has suggested, ancestors of the cynomolgus macaque lived in Sundaland, which was created by sea-level lowering during the glacial period [17,36]. The most recent population bottleneck around 20,000 years ago may correspond to the last glacial maximum, when average temperatures were 2 to 6°C lower than the present temperatures. The change in population